

Tetraalkoxyaluminates of Nickel(II), Copper(II), and Copper(I)

Michael Veith,^{*,†,‡} Kroum Valtchev,[†] and Volker Huch[†]Institute of Inorganic Chemistry, Saarland University, Saarbruecken, Germany, and
Leibniz-Institut fuer Neue Materialien (INM), Saarbruecken, Germany

Received September 3, 2007

The syntheses and structural details of tetraisopropoxyaluminates and tetra-*tert*-butoxyaluminates of nickel(II), copper(I), and copper(II) are reported. Within the nickel series, either $\text{Ni}[\text{Al}(\text{O}^i\text{Pr})_4]_2 \cdot 2\text{HO}^i\text{Pr}$, with nickel(II) in a distorted octahedral oxygen environment, or $\text{Ni}[\text{Al}(\text{O}^i\text{Pr})_4]_2 \cdot \text{py}$, with nickel(II) in a square-pyramidal O_4N coordination sphere, or $\text{Ni}[(^i\text{PrO})(^t\text{BuO})_3\text{Al}]_2$, with Ni(II) in a quasi-tetrahedral oxygen coordination, has been obtained. Another isolated complex is $\text{Ni}[(^i\text{PrO})_3\text{AlOAl}(\text{O}^i\text{Pr})_3] \cdot 3\text{py}$ (with nickel(II) being sixfold-coordinated), which may also be described as a “NiO” species trapped by two $\text{Al}(\text{O}^i\text{Pr})_3$ Lewis acid–base systems stabilized at nickel by three pyridine donors. Copper(I) compounds have been isolated in three forms: $[(^i\text{PrO})_4\text{Al}]\text{Cu} \cdot 2\text{py}$, $[(^t\text{BuO})_4\text{Al}]\text{Cu} \cdot 2\text{py}$, and $\text{Cu}_2[(^t\text{BuO})_4\text{Al}]_2$. In all of these compounds, the aluminate moiety behaves as a bidentate unit, creating a tetrahedrally distorted N_2O_2 copper environment in the pyridine adducts. In the base-free copper(I) *tert*-butoxyaluminate, a dicopper dumbbell [$\text{Cu} \cdots \text{Cu}$ 2.687(1) Å] is present with two oxygen contacts on each of the copper atoms. Copper(II) alkoxyaluminates have been characterized either as $\text{Cu}[(^t\text{BuO})_4\text{Al}]_2$, $\{\text{Cu}(^i\text{PrO})[(^i\text{PrO})_4\text{Al}]\}_2$, and $\text{Cu}[(^t\text{BuO})_3(^i\text{PrO})\text{Al}]_2$ (copper being tetracoordinated by oxygen) or as $[(^i\text{PrO})_4\text{Al}]_2\text{Cu} \cdot \text{py}$ (pentacoordinated copper similar to the nickel derivative). Finally, a copper(II) hydroxyaluminate has been isolated, displaying pentacoordinate copper (O_4N coordination sphere) by dimerization, with the formula $\{[(^t\text{BuO})_4\text{Al}]\text{Cu}(\text{OH}) \cdot \text{py}\}_2$. The formation of all of these isolated products is not always straightforward because some of these compounds in solution are subject to decomposition or are involved in equilibria. Besides NMR [copper(I) compounds], UV absorptions and magnetic moments are used to characterize the compounds.

Introduction

Since the pioneering work carried out by Meerwein and Bersin,¹ the field of heterometallic alkoxides has been rapidly growing.² The increasing interest is due to their potential application as precursors for oxide-based ceramic materials using either sol–gel³ or chemical vapor deposition (CVD) techniques.⁴

Double alkoxides of bivalent late transition metals with aluminum(III) represented by the general formula $\text{M}[\text{Al}(\text{OR})_4]_2$ [where $\text{M} = \text{Mn}^{\text{II}}, \text{Fe}^{\text{II}}, \text{Co}^{\text{II}}, \text{Ni}^{\text{II}},$ and Cu^{II} and $\text{R} = \text{Me}, \text{Et}, ^i\text{Pr},$ and O^tBu] were synthesized by Mehrotra and co-workers.⁵ Predictions of the structural features of the heterometallic alkoxides were made on the basis of spectroscopic and magnetic measurements.⁶ The alkoxy anions $[\text{Al}(\text{OR})_4]^-$ have been reported to behave as ambidentate ligands depending on the nature of the central metal atom and on the steric bulk of the alkoxy group involved. In view of that mentioned above, it is of considerable interest to explore the chemistry and bonding characteristics of the tetraalkoxyaluminates with respect to the later 3d metals.

* To whom correspondence should be addressed. E-mail: veith@mx.uni-saarland.de.

† Saarland University.

‡ INM.

- (1) Meerwein, H.; Bersin, T. *Liebigs Ann. Chem.* **1929**, 476, 113–150.
- (2) (a) Veith, M.; Mathur, S.; Mathur, Ch. *Polyhedron* **1998**, 17, 1005–1034. (b) Mehrotra, R. C.; Singh, A.; Sogani, S. *Chem. Rev.* **1994**, 94, 1643–1660. (c) Mehrotra, R. C.; Singh, A.; Sogani, S. *Chem. Soc. Rev.* **1994**, 215–225. (d) Caulton, K. G.; Hubert-Pfalzgraf, L. G. *Chem. Rev.* **1990**, 90, 969–995.
- (3) Mehrotra, R. C. *Chemtracts: Anal., Phys., Inorg. Chem.* **1990**, 2, 389–399.
- (4) (a) Jones, A. C. *Chem. Vap. Deposition* **1998**, 4, 169–179. (b) Herrmann, W. A.; Huber, N. W.; Runte, O. *Angew. Chem.* **1995**, 107, 2371–2390.

- (5) (a) Singh, J. V.; Jain, N. C.; Mehrotra, R. C. *Synth. React. Inorg. Met.-Org. Chem.* **1979**, 9 (1), 79–88. (b) Garg, G.; Dubey, R. K.; Singh, A.; Mehrotra, R. C. *Polyhedron* **1991**, 10, 1733–1739.
- (6) (a) Mehrotra, R. C.; Singh, J. *Can. J. Chem.* **1984**, 62, 1003–1007. (b) Mehrotra, R. C.; Singh, J. V. *Z. Anorg. Allg. Chem.* **1984**, 512, 221–230. (c) Stampf, E.; Hillebrand, U. *Z. Naturforsch.* **1979**, 34b, 262–265.

Table 1. Crystal Data and Structure Solution Parameters of Compounds **4**, **5**, **7**, and **9–11**

compound	4	5	7	9	10	11
empirical formula	C ₃₀ H ₇₂ Al ₂ NiO ₁₀	C ₂₉ H ₆₁ Al ₂ NNiO ₈	C ₃₃ H ₅₇ Al ₂ N ₃ NiO ₇	C ₃₀ H ₇₀ Al ₂ Cu ₂ O ₁₀	C ₂₉ H ₆₁ Al ₂ CuNO ₈	C ₂₂ H ₃₈ AlCuN ₂ O ₄
fw	705.55	664.46	720.49	771.90	669.29	485.06
cryst syst	orthorhombic	monoclinic	monoclinic	monoclinic	monoclinic	orthorhombic
space group	<i>Pbca</i>	<i>P2₁/c</i>	<i>C2/c</i>	<i>P2₁/n</i>	<i>P2₁</i>	<i>Pccn</i>
unit cell dimens:						
<i>a</i> (Å)	10.678(2)	13.084(3)	12.034(2)	10.178(2)	9.250(2)	17.064(3)
<i>b</i> (Å)	18.222(4)	17.054(3)	16.732(3)	16.774(3)	16.373(3)	9.400(2)
<i>c</i> (Å)	44.127(9)	17.805(4)	17.281(3)	12.956(3)	13.473(3)	16.945(3)
α (deg)						
β (deg)		97.81(3)	95.25(3)	93.36(3)	99.41(3)	
γ (deg)						
<i>V</i> (Å ³)	8586(3)	3936(2)	3465(1)	2208.1(8)	2013.0(7)	2718.0(9)
<i>Z</i>	8	4	4	2	2	4
density _{calc} (Mg/m ³)	1.092	1.121	1.381	1.161	1.104	1.185
abs coeff (mm ⁻¹)	0.535	0.577	0.661	1.044	0.625	0.862
<i>F</i> (000)	3088	1440	1544	828	722	1032
cryst size (mm ³)	0.5 × 0.44 × 0.2	0.6 × 0.45 × 0.3	0.4 × 0.35 × 0.2	0.60 × 0.19 × 0.12	0.5 × 0.35 × 0.28	0.3 × 0.25 × 0.15
θ range for data collcn	2–18.52	1.6–22.56	2–24.94	2.43–24.02	1.53–22.45	2.7–24.15
reflns collected	18 234	5154	11 141	13 309	2693	16 000
indep reflns	3122	3740	2821	3311	2693	2040
[<i>I</i> > 2 σ (<i>I</i>)]						
data/param	3122/388	5154/370	2821/210	3311/218	2693/370	2040/137
GOF in <i>F</i> ²	1.045	1.055	0.970	0.997	1.130	1.025
final <i>R</i> indices (wR2)	0.059 (0.145)	0.061 (0.146)	0.070 (0.18)	0.047 (0.123)	0.047 (0.138)	0.064 (0.17)
[<i>I</i> > 2 σ (<i>I</i>)]						
<i>R</i> indices (all data)	0.081 (0.161)	0.091 (0.173)	0.093 (0.20)	0.074 (0.134)	0.055 (0.153)	0.099 (0.19)
largest diff peak and hole (e/Å ³)	0.336 and –0.222	0.386 and –0.283	0.590 and –0.346	0.390 and –0.326	0.318 and –0.237	0.352 and –0.350

The preparation of mixed-metal oxides with spinel structures using either a sol–gel or microemulsion-mediated sol–gel process has been the subject of several papers.⁷ We were exploring the possibility of using these compounds as single-source precursors in a CVD process. In the course of our investigations, we were faced with a series of problems concerning the preparation and, in particular, the purification of the compounds. Furthermore, the double isopropoxides appeared to partly decompose upon distillation. As a result of this, the metal content of the materials obtained by the CVD process varied significantly in the expected values. In order to gain insight into the behavior of the mixed-metal alkoxides, which is necessary for control of the CVD process, the present study was undertaken.

This paper is concerned with the synthesis and structural characterization of the heterometallic alkoxides of nickel(II) and copper(II) containing [Al(OR)₄][–] groups (R = OⁱPr and O^tBu). Our interest was focused on their thermal stability and, in particular, on the decomposition of the isopropoxides upon vaporization. To the best of our knowledge, there is no example of copper(I) aluminates reported in the literature so far. Therefore, this work was later extended to the synthesis and characterization of the corresponding copper(I) derivatives.

Experimental Section

General Comments. All operations were carried out under an atmosphere of purified and dry nitrogen using a modified Stock apparatus. All solvents were dried by distillation from sodium. The hydrocarbon solvents were stored over sodium, isopropyl alcohol, *tert*-butanol, and pyridine over molecular sieves. Al(OⁱPr)₃ and Al-

(O^tBu)₃ were prepared by the reaction of aluminum metal with isopropyl alcohol and *tert*-butanol, respectively, following a published procedure.⁸ Anhydrous nickel(II), copper(II), and copper(I) chlorides were prepared by literature methods.⁹

Physical Methods. ¹H and ¹³C NMR were obtained on a Bruker AC-200 spectrometer, and chemical shifts were referenced to solvent resonances. Magnetic moments in solution were measured by the Evans method¹⁰ and were adjusted for diamagnetic contributions using Pascal's constants. The LECO CHN 900 elemental analyzer was used for elemental analyses. UV–vis spectra were recorded on a Pye Unicam SP8-100 or a Perkin-Elmer Lambda 35. The metal contents of the new compounds were obtained by titrimetric procedures.

Crystallography. Diffraction intensities were collected on a Stoe IPDS or Siemens Stoe AED 2 diffractometer equipped with graphite-monochromated Mo K α radiation. The structures were solved by direct methods and refined with the full-matrix least squares on *F*² using the *SHELXS-97* and *SHELXL-97* programs.¹¹ Anisotropic thermal parameters were assigned to all non-H atoms. The H atoms were generated geometrically. The crystallographic data are summarized in Tables 1 and 2. Selected bond lengths and angles for **4**, **5**, **7**, **9–11**, and **12–17** are listed in Tables 3 and 4. Full data are available upon request.

- (7) (a) Otero Arean, C.; Penarroya Mentrut, M.; Lopez Lopez, A. J.; Parra, J. B. *Colloids Surf. A* **2001**, *180* (3), 253–258. (b) Escalona Platero, E.; Otero Arean, C.; Parra, J. B. *Res. Chem. Intermed.* **1999**, *25* (2), 187–194. (c) Meyer, F.; Hempelmann, R.; Mathur, S.; Veith, M. J. *Mater. Chem.* **1999**, *9*, 1755–1763.
- (8) Adkins, H. *J. Am. Chem. Soc.* **1922**, *44*, 2175–2180.
- (9) Brauer, G. *Handbuch der Praeparativen Anorganischen Chemie*; Ferdinand Enke Verlag: Stuttgart, Germany, 1978.
- (10) Evans, D. F. *J. Chem. Soc.* **1959**, 2003–2005.
- (11) (a) Sheldrick, G. M. *SHELXS-97, Program for Crystal Structure Solution*; University of Göttingen: Göttingen, Germany, 1997. (b) Sheldrick, G. M. *SHELXL-97, Program for Crystal Structure Determination*; University of Göttingen: Göttingen, Germany, 1997.

Table 2. Crystal Data and Structure Solution Parameters of Compounds **12**–**17**

compound	12	13	14	15	16	17
empirical formula	C ₃₀ H ₆₈ Al ₂ CuO ₈	C ₃₀ H ₆₈ Al ₂ NiO ₈	C ₃₂ H ₇₂ Al ₂ CuO ₈	C ₂₆ H ₄₆ AlCuN ₂ O ₄	C ₃₂ H ₇₂ Al ₂ Cu ₂ O ₈	C ₄₂ H ₈₄ Al ₂ Cu ₂ N ₂ O ₁₀
fw	674.34	669.51	702.40	541.17	765.94	958.15
cryst syst	monoclinic	orthorhombic	monoclinic	triclinic	triclinic	triclinic
space group	<i>P</i> 2 ₁ / <i>n</i>	<i>P</i> 2 ₁ 2 ₁ 2 ₁	<i>P</i> 2 ₁ / <i>n</i>	<i>P</i> 1	<i>P</i> 1	<i>P</i> 1
unit cell dimens:						
<i>a</i> (Å)	9.976(2)	9.317(2)	10.068(2)	9.820(2)	9.536(2)	10.275(2)
<i>b</i> (Å)	16.361(3)	17.258(3)	16.493(3)	11.993(2)	10.209(2)	10.668(2)
<i>c</i> (Å)	25.451(5)	26.922(5)	25.809(5)	13.846(3)	11.387(2)	13.277(3)
α (deg)				83.03(3)	96.91(3)	75.40(3)
β (deg)	92.29(3)		93.05(3)	73.62(3)	103.95(3)	74.85(3)
γ (deg)				81.39(3)	96.40(3)	79.11(3)
<i>V</i> (Å ³)	4150.7(14)	4328.9(14)	4280(1)	1541.5(5)	1056.6(4)	1347.6(5)
<i>Z</i>	4	4	4	2	1	1
density _{calc} (Mg/m ³)	1.079	1.027	1.090	1.166	1.204	1.181
abs coeff (mm ^{−1})	0.606	0.524	0.590	0.766	1.088	0.870
<i>F</i> (000)	1468	1464	1532	580	412	514
cryst size (mm ³)	0.5 × 0.4 × 0.35	0.4 × 0.1 × 0.08	0.8 × 0.4 × 0.3	0.4 × 0.35 × 0.2	0.3 × 0.22 × 0.2	0.5 × 0.4 × 0.28
θ range for data collcn	2.63–24.22	1.51–24.00	1.6–22.50	1.54–22.50	1.86–23.97	2.63–23.96
reflns collected	22 740	3841	5584	4031	6600	8237
indep reflns	6574	3841	4376	3430	3075	3863
[<i>I</i> > 2 σ (<i>I</i>)]						
data/param	6574/370	3841/445	5584/388	4031/363	3075/199	3863/157
GOF in <i>F</i> ²	0.953	1.123	1.071	1.104	1.082	1.77
final <i>R</i> indices	0.079 (0.219)	0.076 (0.164)	0.067 (0.18)	0.045 (0.117)	0.031 (0.083)	0.096 (0.261)
(wR2)						
[<i>I</i> > 2 σ (<i>I</i>)]						
<i>R</i> indices (all data)	0.12 (0.25)	0.13 (0.21)	0.088 (0.20)	0.056 (0.128)	0.038 (0.098)	0.11 (0.27)
largest diff peak and hole (e/Å ³)	0.771 and −0.282	0.339 and −0.180	0.621 and −0.340	0.232 and −0.404	0.362 and −0.233	2.038 and −0.701

Syntheses and Reactions. {Ni[Al(O^{*i*}Pr)₄]₂} (**1**). A solution of K[Al(O^{*i*}Pr)₄], prepared by the reaction of potassium metal (2.46 g, 62.8 mmol) in isopropyl alcohol (100 mL) and Al(O^{*i*}Pr)₃ (12.83 g, 62.82 mmol), was added to a suspension of NiCl₂ (4.071 g, 31.41 mmol) in isopropyl alcohol (20 mL). The reaction mixture was refluxed for 20 h for the completion of the reaction. Toluene (50 mL) was added to the mixture, and the precipitated KCl was removed by filtration. The solvent was evaporated off under reduced pressure, and the remaining violet liquid was filtered once again to remove the last solid residues. Yield of crude product: 15.63 g (85%). The vacuum distillation (90 °C, 10^{−3} mbar) yielded 11.95 g (65%) of **1** as a violet liquid, which contains a small amount of Al(O^{*i*}Pr)₃ (1–2%). Compound **1** could be obtained in a pure form as a crystalline solid after removal of the solvent from {Ni[Al(O^{*i*}Pr)₄]₂·2HO^{*i*}Pr} (**4**) in vacuum (50 °C, 10^{−3} mbar). Anal. Calcd for C₂₈H₅₆Al₂NiO₈: C, 49.24; H, 9.64; Al, 9.22; Ni, 10.03. Found: C, 48.50; H, 9.78; Al, 9.78; Ni, 9.86. UV–vis [cyclohexane; λ_{max} , nm (ϵ , M^{−1} cm^{−1}): 424 (24), 525 (111), 578 (97), 781 (11), 819 (12). Magnetic moment obtained by the Evans method (C₆H₆/C₆D₆): 3.19 μ_{B} .

{(PrO)Ni[Al(O^{*i*}Pr)₄]₂} (**3**). **1** (3.64 g, 6.22 mmol) was allowed to reflux for approximately 70 h, yielding 0.90 g of **3** as blue solid residue. The obtained sublimate, which consisted of **1** and Al(O^{*i*}Pr)₃, was re-treated in the same way to yield a second crop of 0.48 g of **3** (total yield: 58%). Anal. Calcd for C₃₀H₇₀Al₂Ni₂O₁₀: C, 47.24; H, 9.25; Al, 7.08; Ni, 15.39. Found: C, 47.59; H, 9.14; Al, 7.21; Ni, 15.70. UV–vis [cyclohexane; λ_{max} , nm (ϵ , M^{−1} cm^{−1}): 440 (59), 531 (244), 588 (200), 787 (22), 820 (26). EI-MS (90 eV, *m/e*): 745 [M − CH₃]⁺, 642 [M − O^{*i*}Pr]⁺, 627 [M − O^{*i*}Pr − CH₃]⁺, 583 [M − O^{*i*}Pr − O^{*i*}Pr]⁺, 569 [M − Ni(O^{*i*}Pr)₂ − CH₃]⁺. Magnetic moment obtained by the Evans method (C₆H₁₂/C₆D₆): 3.41 μ_{B} .

{Ni[Al(O^{*i*}Pr)₄]₂·2HO^{*i*}Pr} (**4**). **1** (4.10 g, 7.00 mmol) was dissolved in isopropyl alcohol (10 mL), whereupon the color of

the solution changed from violet to yellow. Upon cooling at ambient temperature, yellow crystals of **4** were formed. The first crop (2.156 g) was isolated by filtration, and the filtrate was concentrated to yield a second crop (1.161 g). Total yield: 67%. Anal. Calcd for C₃₀H₇₂Al₂NiO₁₀: C, 51.07; H, 10.29; Al, 7.65; Ni, 8.32. Found: C, 51.21; H, 10.52; Al, 7.63; Ni, 8.34. UV–vis (isopropyl alcohol; λ_{max} , nm (ϵ , M^{−1} cm^{−1}): 786 (3.5), 733 (sh, 2.5), 423 (16). Magnetic moment obtained by the Evans method (C₆H₆/HO^{*i*}Pr/C₆D₆): 3.25 μ_{B} .

{Ni[Al(O^{*i*}Pr)₄]₂·py} (**5**). Equimolar reaction between **1** and pyridine in toluene yielded a dark-yellow oil, which crystallized slowly at ambient temperature. Anal. Calcd for C₂₉H₆₁Al₂NNiO₈: C, 52.42; H, 9.25; N, 2.11; Al, 8.12; Ni, 8.83. Found: C, 52.62; H, 9.61; N, 1.96; Al, 7.71; Ni, 8.69. UV–vis [toluene; λ_{max} , nm (ϵ , M^{−1} cm^{−1}): 782, 739, 599, 504, 424 (54). Magnetic moment obtained by the Evans method (C₆H₅CH₃/C₆D₆): 3.18 μ_{B} .

{Ni[Al(O^{*i*}Pr)₄]₂·2py} (**6**) was prepared by the reaction of **1** with an excess of pyridine used as a solvent. Upon concentration, green crystals from **6** formed. Anal. Calcd for C₃₄H₆₆Al₂N₂NiO₈: C, 54.92; H, 8.95; N, 3.77; Al, 7.26; Ni, 7.89. Found: C, 55.86; H, 9.13; N, 3.55; Al, 6.16; Ni, 7.11. UV–vis [toluene; λ_{max} , nm (ϵ , M^{−1} cm^{−1}): 756 (3), 691 (sh), 406 (10).

[NiOAl₂(O^{*i*}Pr)₆·3py] (**7**) was obtained as a side product by the synthesis of **6** when water residues were present in the solvent. For analysis, blue crystals were selected from the mixture of crystals. Anal. Calcd for C₃₃H₅₇Al₂N₃NiO₇: C, 55.01; H, 7.97; N, 5.83. Found: C, 54.83; H, 8.05; N, 5.62.

{Cu[Al(O^{*i*}Pr)₄]₂} (**2**) was prepared analogously to **1** by the reaction of anhydrous CuCl₂ (4.73 g, 35.1 mmol) and K[Al(O^{*i*}Pr)₄] prepared by the reaction of potassium metal (2.75 g, 70.3 mmol) in isopropyl alcohol (100 mL) and Al(O^{*i*}Pr)₃ (14.36 g, 70.3 mmol). Yield: 19.47 g (94%) of a viscous bluish-green liquid. The distillation at 95 °C and 2 × 10^{−2} mbar is accompanied by decomposition, yielding an impure product. For this reason, **2** was

Table 3. Selected Bond Lengths (Å) and Angles (deg) for **4**, **5**, **7**, and **9–11**

{Ni[Al(O ⁱ Pr) ₄] ₂ ·2HO ⁱ Pr} (4)					
Ni1–O1	2.039(5)	O1–Ni1–O4	94.6(2)	O8–Al2–O7	112.3(3)
Ni1–O4	2.055(5)	O1–Ni1–O2	73.4(2)	O8–Al2–O4	120.7(3)
Ni1–O2	2.059(5)	O4–Ni1–O2	99.1(2)	O7–Al2–O4	106.7(3)
Ni1–O3	2.061(5)	O1–Ni1–O3	98.6(2)	O8–Al2–O3	118.8(3)
Ni1–O10	2.093(5)	O4–Ni1–O3	73.2(2)	O7–Al2–O3	107.1(3)
Ni1–O9	2.124(5)	O2–Ni1–O3	168.7(2)	O4–Al2–O3	88.5(2)
Al2–O8	1.652(7)	O1–Ni1–O10	86.9(2)	O6–Al1–O5	113.5(3)
Al2–O7	1.733(6)	O4–Ni1–O10	173.9(2)	O6–Al1–O1	120.6(3)
Al2–O4	1.750(5)	O2–Ni1–O10	87.0(2)	O5–Al1–O1	106.5(3)
Al2–O3	1.765(5)	O3–Ni1–O10	100.7(2)	O6–Al1–O2	118.0(3)
Al1–O6	1.659(7)	O1–Ni1–O9	176.0(2)	O5–Al1–O2	106.9(3)
Al1–O5	1.711(6)	O4–Ni1–O9	87.5(2)	O1–Al1–O2	88.2(2)
Al1–O1	1.750(5)	O2–Ni1–O9	103.0(2)	Al1···Ni1···Al2	138.14(8)
Al1–O2	1.766(5)	O3–Ni1–O9	85.2(2)		
Ni1···Al1	2.851(2)				
Ni1···Al2	2.857(3)				
{Ni[Al(O ⁱ Pr) ₄] ₂ ·py} (5)					
Ni1–O4	1.991(3)	Ni1···Al2	2.884(2)	O6–Al1–O1	113.0(2)
Ni1–O1	1.996(3)	Ni1···Al1	2.893(2)	O5–Al1–O1	109.5(2)
Ni1–N1	2.001(5)	O4–Ni1–O1	141.5(2)	O6–Al1–O2	111.0(2)
Ni1–O3	2.050(3)	O4–Ni1–N1	111.9(2)	O5–Al1–O2	113.2(2)
Ni1–O2	2.054(3)	O1–Ni1–N1	106.6(2)	O1–Al1–O2	87.5(2)
Al1–O6	1.666(5)	O4–Ni1–O3	74.6(1)	O8–Al2–O7	115.1(3)
Al1–O5	1.676(4)	O1–Ni1–O3	102.3(1)	O8–Al2–O3	114.6(3)
Al1–O1	1.772(4)	N1–Ni1–O3	94.1(2)	O7–Al2–O3	111.6(2)
Al1–O2	1.774(4)	O4–Ni1–O2	101.5(1)	O8–Al2–O4	115.1(3)
Al2–O8	1.642(5)	O1–Ni1–O2	74.5(1)	O7–Al2–O4	109.7(2)
Al2–O7	1.687(5)	N1–Ni1–O2	96.4(2)	O3–Al2–O4	87.6(2)
Al2–O3	1.762(4)	O3–Ni1–O2	169.5(1)	Al2···Ni1···Al1	149.86(6)
Al2–O4	1.775(4)	O6–Al1–O5	118.6(2)		
{NiAl ₂ O(O ⁱ Pr) ₆ ·3py} (7)					
Ni1–O4	1.990(4)	O4–Ni1–N2	180.000(1)	N2–Ni1–O1'	104.09(9)
Ni1–N2	2.014(5)	O4–Ni1–N1	92.3(1)	O1–Ni1–O1'	151.8(2)
Ni1–N1	2.021(4)	N2–Ni1–N1	87.8(1)	O2–Al1–O3	106.6(2)
Ni1–O1	2.025(3)	N1'–Ni1–N1	175.5(2)	O2–Al1–O4	117.3(2)
Al1–O2	1.624(3)	O4–Ni1–O1	75.91(9)	O3–Al1–O4	117.5(2)
Al1–O3	1.642(3)	N2–Ni1–O1	104.09(9)	O2–Al1–O1	116.3(2)
Al1–O4	1.676(1)	N1'–Ni1–O1	87.4(1)	O3–Al1–O1	105.3(2)
Al1–O1	1.726(3)	N1–Ni1–O1	93.7(1)	O4–Al1–O1	93.1(2)
Ni1···Al1	2.752(2)	O4–Ni1–O1'	75.91(9)		
{(iPrO)Cu[Al(O ⁱ Pr) ₄] ₂ ·py} (9)					
Cu–O1	1.918(3)	O1–Cu–O1'	82.0(1)	O5–Al–O2	116.2(2)
Cu–O1'	1.921(3)	O1–Cu–O3	104.3(1)	O4–Al–O2	115.0(2)
Cu–O3	1.947(3)	O1'–Cu–O3	160.1(1)	O5–Al–O3	116.4(2)
Cu–O2	1.951(3)	O1–Cu–O2	158.7(1)	O4–Al–O3	116.0(2)
Al–O5	1.675(4)	O1'–Cu–O2	104.1(1)	O2–Al–O3	85.1(1)
Al–O4	1.685(4)	O3–Cu–O2	77.0(1)		
Al–O2	1.793(3)	O5–Al–O4	107.3(3)		
Al–O3	1.794(3)				
Cu···Al	2.846(1)				
Cu···Cu'	2.898(1)				
{Cu[Al(O ⁱ Pr) ₄] ₂ ·py} (10)					
Cu1–O1	1.964(5)	Cu1···Al1	2.854(2)	O7–Al1–O4	113.6(3)
Cu1–O3	1.973(5)	Cu1···Al2	2.956(3)	O5–Al1–O1	117.2(3)
Cu1–O4	1.976(5)	O1–Cu1–O3	170.3(2)	O7–Al1–O1	110.7(3)
Cu1–N1	2.020(7)	O1–Cu1–O4	76.7(2)	O4–Al1–O1	85.9(2)
Cu1–O2	2.316(6)	O3–Cu1–O4	96.6(2)	O6–Al2–O8	114.3(5)
Al1–O5	1.695(6)	O1–Cu1–N1	92.0(3)	O6–Al2–O2	110.0(4)
Al1–O7	1.706(7)	O3–Cu1–N1	92.1(2)	O8–Al2–O2	115.6(5)
Al1–O4	1.780(6)	O4–Cu1–N1	158.7(3)	O6–Al2–O3	109.9(4)
Al1–O1	1.809(6)	O1–Cu1–O2	115.2(2)	O8–Al2–O3	113.1(4)
Al2–O6	1.687(9)	O3–Cu1–O2	72.7(2)	O2–Al2–O3	91.7(3)
Al2–O8	1.692(8)	O4–Cu1–O2	100.8(3)	Al1···Cu1···Al2	133.63(8)
Al2–O2	1.754(6)	N1–Cu1–O2	100.3(3)		
Al2–O3	1.807(6)	O5–Al1–O7	111.6(3)		
		O5–Al1–O4	115.6(3)		
{Cu[Al(O ⁱ Pr) ₄] ₂ ·2py} (11)					
Cu1–N1	1.945(4)	N1–Cu1–N1'	145.9(3)	O2–Al1–O2'	103.0(3)
Cu1–O1	2.312(3)	N1–Cu1–O1	108.4(2)	O2–Al1–O1'	116.3(2)
Al1–O2	1.720(4)	N1–Cu1–O1'	00.0(2)	O2–Al1–O1	113.7(2)
Al1–O1	1.736(3)	O1–Cu1–O1'	67.0(2)	O1'–Al1–O1	94.6(2)

Table 4. Selected Bond Lengths (Å) and Angles (deg) for **12–17**

{Cu[Al(O ⁱ Pr)(O ⁱ Bu) ₃] ₂ } (12)					
Cu1–O2	1.918(4)	O2–Cu1–O1	119.4(2)	O5–Al1–O1	112.1(3)
Cu1–O1	1.926(4)	O2–Cu1–O4	139.0(2)	O4–Al1–O1	86.0(2)
Cu1–O4	1.927(4)	O1–Cu1–O4	78.0(2)	O8–Al2–O7	119.3(5)
Cu1–O3	1.929(4)	O2–Cu1–O3	77.9(2)	O8–Al2–O3	112.8(4)
Al1–O6	1.631(6)	O1–Cu1–O3	138.2(2)	O7–Al2–O3	111.4(3)
Al1–O5	1.637(6)	O4–Cu1–O3	115.1(2)	O8–Al2–O2	110.8(4)
Al1–O4	1.768(4)	O6–Al1–O5	119.5(4)	O7–Al2–O2	112.0(3)
Al1–O1	1.789(4)	O6–Al1–O4	110.1(4)	O3–Al2–O2	85.7(2)
Al2–O8	1.624(7)	O5–Al1–O4	114.0(3)	Al1···Cu1···Al2	174.93(6)
Al2–O7	1.637(5)	O6–Al1–O1	110.2(3)		
Al2–O3	1.771(4)				
Al2–O2	1.784(4)				
Cu1···Al1	2.795(2)				
Cu1···Al2	2.800(2)				
{Ni[Al(O ⁱ Pr)(O ⁱ Bu) ₃] ₂ } (13)					
Ni–O1	1.939(7)	O1–Ni–O2	77.1(3)	O2–Al1–O1	84.9(3)
Ni–O2	1.938(7)	O1–Ni–O4	129.7(3)	O7–Al2–O8	117.3(7)
Ni–O4	1.951(7)	O2–Ni–O4	129.4(3)	O7–Al2–O3	112.5(5)
Ni–O3	1.954(7)	O1–Ni–O3	126.0(3)	O8–Al2–O3	112.2(6)
Al1–O5	1.65(1)	O2–Ni–O3	125.1(3)	O7–Al2–O4	114.0(5)
Al1–O6	1.67(1)	O4–Ni–O3	77.5(3)	O8–Al2–O4	110.8(6)
Al1–O2	1.772(7)	O5–Al1–O6	119.4(7)	O3–Al2–O4	85.8(3)
Al1–O1	1.805(8)	O5–Al1–O2	110.3(5)	Al1···Ni···Al2	173.3(1)
Al2–O7	1.63(1)	O6–Al1–O2	113.1(5)		
Al2–O8	1.64(1)	O5–Al1–O1	111.7(5)		
Al2–O3	1.789(7)	O6–Al1–O1	112.3(5)		
Al2–O4	1.802(8)				
Ni···Al1	2.831(3)				
Ni···Al2	2.838(3)				
{Cu[Al(O ⁱ Bu) ₄] ₂ } (14)					
Cu1–O4	1.930(3)	O4–Cu1–O2	134.1(2)	O6–Al1–O1	111.3(3)
Cu1–O2	1.935(3)	O4–Cu1–O3	118.8(2)	O4–Al1–O1	85.6(2)
Cu1–O3	1.941(3)	O2–Cu1–O3	77.6(2)	O8–Al2–O7	118.5(4)
Cu1–O1	1.943(3)	O4–Cu1–O1	77.8(1)	O8–Al2–O3	113.4(3)
Al1–O5	1.644(5)	O2–Cu1–O1	124.0(1)	O7–Al2–O3	111.7(3)
Al1–O6	1.648(5)	O3–Cu1–O1	133.4(1)	O8–Al2–O2	110.7(3)
Al1–O4	1.787(4)	O5–Al1–O6	119.1(3)	O7–Al2–O2	112.3(3)
Al1–O1	1.794(3)	O5–Al1–O4	113.7(3)	O3–Al2–O2	85.8(2)
Al2–O8	1.637(5)	O6–Al1–O4	110.0(3)	Al2···Cu1···Al1	173.71(5)
Al2–O7	1.643(4)	O5–Al1–O1	112.3(2)		
Al2–O3	1.778(4)				
Al2–O2	1.788(4)				
Cu1···Al2	2.815(2)				
Cu1···Al1	2.816(2)				
{Cu[Al(O ⁱ Bu) ₄] ₂ ·2py} (15)					
Cu1–N1	1.949(3)	N1–Cu1–N2	137.4(1)	O4–Al1–O3	109.8(1)
Cu1–N2	1.968(3)	N1–Cu1–O1	112.0(1)	O4–Al1–O1	117.2(1)
Cu1–O1	2.232(2)	N2–Cu1–O1	102.9(1)	O3–Al1–O1	109.5(1)
Cu1–O2	2.246(2)	N1–Cu1–O2	111.8(1)	O4–Al1–O2	116.9(1)
Al1–O4	1.708(2)	N2–Cu1–O2	102.9(1)	O3–Al1–O2	109.6(1)
Al1–O3	1.715(2)	O1–Cu1–O2	69.17(8)	O1–Al1–O2	92.6(1)
Al1–O1	1.756(2)				
Al1–O2	1.759(2)				
Cu1···Al1	2.991(1)				
{CuAl(O ⁱ Bu) ₄] ₂ } (16)					
Cu1–O2	1.884(2)	Al1–O3	1.691(2)	O2–Cu1–O1	176.44(7)
Cu1–O1	1.889(2)	Al1–O4	1.715(2)	O3–Al1–O4	120.4(1)
Cu1–Cu1'	2.687(1)	Al1–O2	1.800(2)	O3–Al1–O2	111.5(1)
Cu1···Al1	2.953(1)	Al1–O1	1.802(2)	O4–Al1–O2	106.0(1)
				O3–Al1–O1	113.4(1)
				O4–Al1–O1	102.4(1)
				O2–Al1–O1	101.1(1)
{(HO)Cu[Al(O ⁱ Bu) ₄] ₂ ·2py} (17)					
Cu1–O1'	1.925(7)	O1'–Cu1–O1	78.2(4)	N1–Cu1–O3	95.2(2)
Cu1–O1	1.926(8)	O1'–Cu1–N1	94.6(3)	O2–Cu1–O3	69.8(2)
Cu1–N1	2.016(7)	O1–Cu1–N1	166.8(3)	O5–Al1–O4	111.3(3)
Cu1–O2	2.033(5)	O1'–Cu1–O2	171.7(3)	O5–Al1–O3	117.6(3)
Cu1–O3	2.393(5)	O1–Cu1–O2	93.6(3)	O4–Al1–O3	111.1(3)
Al1–O5	1.707(6)	N1–Cu1–O2	93.2(3)	O5–Al1–O2	115.1(3)
Al1–O4	1.725(6)	O1'–Cu1–O3	111.9(3)	O4–Al1–O2	109.7(3)
Al1–O3	1.762(6)	O1–Cu1–O3	97.7(3)	O3–Al1–O2	90.5(3)
Al1–O2	1.828(5)				
Al1–O2	1.828(5)				

used without further purification. Anal. Calcd for $C_{24}H_{56}Al_2CuO_8$: C, 48.84; H, 9.56; Al, 9.14; Cu, 10.77. Found: C, 49.17; H, 9.25; Al, 9.14; Cu, 10.77. UV-vis [benzene; λ_{\max} , nm]: 714. Magnetic moment obtained by the Evans method (C_6H_6/C_6D_6): 1.75 μ_B .

$\{(\text{PrO})\text{Cu}^{\text{II}}[\text{Al}(\text{O}^i\text{Pr})_4]\}_2$ (**9**). Under prolonged storage, **2** gradually decomposed to **8**, **9**, and aluminum isopropoxide. After a period of 6 months, the compound mixture was filtered, whereupon **9** partly crystallized out from the filtered green oil. For analytical characterization, blue crystals were selected. Anal. Calcd for $C_{30}H_{70}Al_2Cu_2O_{10}$: C, 46.68; H, 9.14. Found: C, 46.43; H, 9.20.

$\{\text{Cu}^{\text{II}}[\text{Al}(\text{O}^i\text{Pr})_3]_2 \cdot \text{py}\}$ (**10**). The reaction of **2** with a slight excess of pyridine resulted in a bluish-green viscous solution. Under storage, blue crystals from **10** were formed. However, small amounts of **11** and aluminum isopropoxide were also present because of the decomposition of **2**, which is even favored by pyridine. For analytical characterization, blue crystals were selected. Anal. Calcd for $C_{29}H_{61}Al_2CuNO_8$: C, 52.04; H, 9.19; N, 2.09. Found: C, 51.79; H, 9.60; N, 1.99.

$\{\text{Cu}^{\text{I}}[\text{Al}(\text{O}^i\text{Pr})_4]_2 \cdot 2\text{py}\}$ (**11**). CuCl (0.836 g, 8.445 mmol) and $K[\text{Al}(\text{O}^i\text{Pr})_4]$ (2.554 g, 8.445 mmol) were dissolved in pyridine (25 mL). The reaction mixture was allowed to reflux for 15 h. After removal of the precipitated KCl by filtration, the solution was concentrated under reduced pressure, whereupon pale-yellow to colorless crystals of **11** were formed (yield: 72%). Anal. Calcd for $C_{22}H_{38}AlCuN_2O_4$: C, 54.47; H, 7.90; N, 5.78; Al, 5.56; Cu, 13.10. Found: C, 54.87; H, 8.19; N, 5.85; Al, 5.58; Cu, 13.14. ^1H NMR (200.1 MHz, C_6D_6 , 294 K): δ 1.31 (d, 24H), 4.44 (sept, 4H). $^{13}\text{C}\{^1\text{H}\}$ NMR (50.3 MHz, C_6D_6 , 294 K): δ 28.58, 63.27.

$\text{Cu}^{\text{I}}[\text{Al}(\text{O}^i\text{Pr})_4]$ (**8**) was obtained in a quantitative yield by the decomposition of **11** at 80 °C in dynamic vacuum. Alternatively, **8** was obtained as a pale-green residue by the thermal decomposition of **2** upon prolonged refluxing. Anal. Calcd for $C_{12}H_{28}AlCuO_4$: C, 44.09; H, 8.63; Al, 8.25; Cu, 19.44. Found: C, 44.07; H, 8.39; Al, 8.33; Cu, 18.58. ^1H NMR (200.1 MHz, C_6D_6 , 294 K): δ 1.44 (d, 24H), 4.57 (sept, 4H). $^{13}\text{C}\{^1\text{H}\}$ NMR (50.3 MHz, C_6D_6 , 294 K): δ 28.59, 63.92. ^{27}Al SPE MAS NMR: δ 59.8. ^{13}C SPE MAS NMR: δ 28.56, 64.89. EI-MS (90 eV, m/e): 652 $[\text{M}]^+$, 594 $[\text{M} - (\text{CH}_3)_2\text{CO}]^+$, 593 $[\text{M} - \text{O}^i\text{Pr}]^+$, 579 $[\text{M} - (\text{CH}_3)_2\text{CO} - \text{CH}_3]^+$.

$\{\text{Cu}^{\text{II}}[\text{Al}(\text{O}^i\text{Pr})(\text{O}^i\text{Bu})_3]_2\}$ (**12**). *tert*-Butanol (25 mL) was added to **2** (5.746 g, 9.736 mmol) dissolved in toluene (25 mL). The solution was stirred overnight at ambient temperature, and then the solvent was removed under reduced pressure. This procedure was repeated several times until the resonances of isopropyl alcohol disappeared from the NMR spectra of the solvent. The final solid was sublimed in vacuum at 120 °C. The sublimate was dissolved in toluene (2 mL), and the solution was filtered in order to remove the insoluble copper(I) aluminum alkoxide species. After evaporation of the volatiles, the residual solid mixture was fractionally sublimed in vacuum at 80, 100, and 120 °C. The sublimate obtained at 120 °C was sublimed again in vacuum at 100 and 120 °C. The second crop (120 °C) was analyzed to be the desired product (yield: 34%). Anal. Calcd for $C_{30}H_{68}Al_2CuO_8$: C, 53.43; H, 10.16; Al, 8.00; Cu, 9.29. Found: C, 53.31; H, 10.28; Al, 8.45; Cu, 9.88. UV-vis [cyclohexane; λ_{\max} , nm (ϵ , $\text{M}^{-1} \text{cm}^{-1}$)]: 850 (80). ^1H NMR (200.1 MHz, C_6D_6 , 294 K): δ 1.1 (br, 36H). $^{13}\text{C}\{^1\text{H}\}$ NMR (50.3 MHz, C_6D_6 , 294 K): δ 35.56, 35.68, 65.2 (br). Magnetic moment obtained by the Evans method (C_6H_6/C_6D_6): 1.83 μ_B .

$\{\text{Ni}[\text{Al}(\text{O}^i\text{Pr})(\text{O}^i\text{Bu})_3]_2\}$ (**13**). *tert*-Butanol (15 mL) was added to **4** (1.149 g, 1.629 mmol) dissolved in toluene (15 mL). The solution was stirred overnight at ambient temperature, and then the solvent was removed under reduced pressure. This procedure was repeated three times until the resonances of isopropyl alcohol disappeared from the NMR spectra of the solvent. Vacuum

sublimation at 120 °C and 10^{-3} bar yielded 1.076 g of **13** (94%). Anal. Calcd for $C_{30}H_{68}Al_2NiO_8$: C, 53.82; H, 10.24; Al, 8.06; Ni, 8.77. Found: C, 53.05; H, 9.98; Al, 8.18; Ni, 8.59. UV-vis [cyclohexane; λ_{\max} , nm]: 432, 535, 577, 806.

$\{\text{Cu}^{\text{II}}[\text{Al}(\text{O}^i\text{Bu})_4]_2\}$ (**14**). A solution of $K[\text{Al}(\text{O}^i\text{Bu})_4]$, prepared by the reaction of KO^{*i*}Bu (0.794 g, 7.08 mmol) in *tert*-butanol (25 mL) with $\text{Al}(\text{O}^i\text{Bu})_3$ (1.744 g, 7.08 mmol) dissolved in toluene (5 mL), was added to a stirred suspension of CuCl₂ (0.476 g, 3.54 mmol) in *tert*-butanol (15 mL). The resulting mixture was refluxed for 10 days to ensure the completion of the reaction. The precipitated KCl was removed by filtration, and the solvent was evaporated off under reduced pressure. Vacuum sublimation at 120 °C gave a mixture of $\text{Al}(\text{O}^i\text{Bu})_3$ and **14**. The two compounds were separated by fractional sublimation. After removal of $[\text{Al}(\text{O}^i\text{Bu})_3]_2$ by heating of the solid mixture at 80 °C and 10^{-3} mbar, the product was sublimed in vacuum at 120 °C, yielding 1.551 g of **14** (64%). Anal. Calcd for $C_{32}H_{72}Al_2CuO_8$: C, 54.72; H, 10.33; Al, 7.68; Cu, 9.05. Found: C, 54.78; H, 10.53; Al, 7.14; Cu, 8.93. UV-vis [cyclohexane; λ_{\max} , nm (ϵ , $\text{M}^{-1} \text{cm}^{-1}$)]: 931 (89). ^1H NMR (200.1 MHz, C_6D_6 , 294 K): δ 1.13 (br, 36H). $^{13}\text{C}\{^1\text{H}\}$ NMR (50.3 MHz, C_6D_6 , 294 K): δ 35.68, 65.3. Magnetic moment obtained by the Evans method (C_6H_6/C_6D_6): 1.94 μ_B .

$\{\text{Cu}^{\text{I}}[\text{Al}(\text{O}^i\text{Bu})_4]_2 \cdot 2\text{py}\}$ (**15**). A solution of $\text{Al}(\text{O}^i\text{Bu})_3$ (2.357 g, 9.57 mmol) in toluene (25 mL) and a solution of KO^{*i*}Bu (2.357 g, 9.57 mmol) in *tert*-butanol (25 mL) and pyridine (5 mL) were subsequently added to CuCl (0.947 g, 9.57 mmol). The resulting mixture was refluxed for 7 days to ensure the completion of the reaction. Filtration of KCl and removal of the solvent under reduced pressure yielded 4.822 g of a crude product (93%). After recrystallization from hot toluene/pyridine (5 mL/1 mL), pale-yellow crystals of **15** were obtained in 77% yield. Alternatively, **15** could be obtained by reacting CuO^{*i*}Bu with $\text{Al}(\text{O}^i\text{Bu})_3$ in a *tert*-butanol/toluene/pyridine solution. Anal. Calcd for $C_{26}H_{46}AlCuN_2O_4$: C, 57.70; H, 8.57; N, 5.18; Al, 4.98; Cu, 11.74. Found: C, 57.68; H, 8.32; N, 5.13; Al, 4.95; Cu, 11.67. ^1H NMR (200.1 MHz, C_6D_6 , 294 K): δ 1.57 (s, 36H). $^{13}\text{C}\{^1\text{H}\}$ NMR (50.3 MHz, C_6D_6 , 294 K): δ 33.96, 68.83.

$\{\text{Cu}^{\text{I}}[\text{Al}(\text{O}^i\text{Bu})_4]_2\}$ (**16**). Upon prolonged heating at 100 °C and 10^{-2} mbar, **15** released pyridine and **16** was formed. The vacuum sublimation of the crude product at 130 °C is accompanied by decomposition, leaving appreciable residue (yield: 64%). The analytically pure colorless product was obtained by recrystallization of the sublimate from hot toluene. Anal. Calcd for $C_{32}H_{72}Al_2Cu_2O_8$: C, 50.18; H, 9.47; Al, 7.05; Cu, 16.59. Found: C, 50.21; H, 9.59; Al, 7.19; Cu, 16.82. ^1H NMR (200.1 MHz, C_6D_6 , 294 K): δ 1.57 (s, 72 H). $^{13}\text{C}\{^1\text{H}\}$ NMR (50.3 MHz, C_6D_6 , 294 K): δ 33.89, 72.21.

$\{(\text{HO})\text{Cu}[\text{Al}(\text{O}^i\text{Bu})_4]_2 \cdot \text{py}\}_2$ (**17**). Crystals of **17** were obtained from a toluene solution of **15** in the presence of air and humidity. Anal. Calcd for $C_{42}H_{84}Al_2Cu_2N_2O_{10}$: C, 52.65; H, 8.84; N, 2.92. Found: C, 52.18; H, 8.32; N, 2.60.

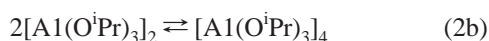
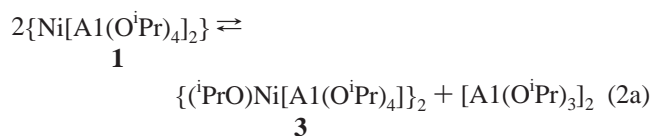
Results and Discussion

Bimetallic isopropoxides containing either nickel(II) or copper(II) and aluminum(III) having the general formula $\{\text{M}[\text{Al}(\text{O}^i\text{Pr})_4]_2\}$ [where M = Ni^{II} (**1**) and Cu^{II} (**2**)] have been prepared according to eq 1 following established routes.^{5a} The mixed-metal alkoxides **1** and **2** were obtained as colored liquids that are highly moisture-sensitive, miscible with nonpolar organic solvents, and volatile. Upon heating under reduced pressure, the compounds tend to undergo partial decomposition, which makes it difficult (in the case of **1**)

and even impossible (in the case of **2**) to isolate the pure double isopropoxides by distillation.

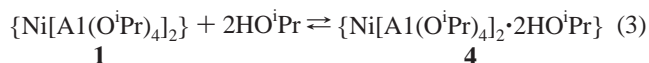


A prolonged refluxing of **1** under reduced pressure induced decomposition, indicated by the release of a white sublimate on the reflux condenser with analytical data corresponding to $[\text{Al}(\text{iPr})_3]_4$. The blue residue in the receiver flask corresponded in analysis to the composition $\text{NiAl}(\text{iPr})_5$ (**3**). Therefore, the following reactions (eqs 2a,b) can be suggested. Both equilibria are continuously shifted to the right because of the gradual crystallization of tetrameric aluminum isopropoxide on the reflux condenser, which results finally in the complete conversion of **1** into **3**. The reversibility of eq 2a was checked by reacting **3** with a stoichiometric amount of aluminum isopropoxide, which indeed led to the formation of **1**. The interconversion reactions of various aluminum isopropoxide oligomers have been extensively studied so far.¹²



In order to investigate possibilities to influence equilibrium (eq 2a), we have studied the interactions of the constituents using strong donor solvents. On the basis of the visible spectra of **1**, Mehrotra and co-workers suggested an equilibrium between tetrahedral and octahedral nickel species in a benzene solution, increasing proportions of octahedral species in an isopropyl alcohol solution, and complete conversion to the octahedral form in pyridine.^{6a} The authors further concluded that the tetraisopropoxyaluminate moieties function both as bidentate and tridentate ligands. By contrast, the investigations carried out in our laboratories do not support such an interpretation. In nonpolar solvents, the nickel coordination environment in **1** appears to be entirely tetrahedral (see further on).

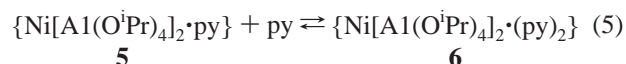
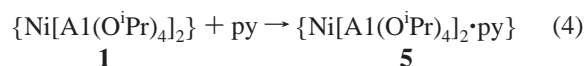
In the case of an isopropyl alcohol solution at room temperature, we found in the UV-vis spectrum between 11 000 and 30 000 cm^{-1} two bands at 12 630 cm^{-1} [ν_2 , ${}^3\text{A}_{2g} \rightarrow {}^3\text{T}_{1g}(\text{F})$] and 23 680 cm^{-1} [ν_3 , ${}^3\text{A}_{2g} \rightarrow {}^3\text{T}_{1g}(\text{P})$], characteristic of hexacoordinated nickel(II), indicating nearly a complete conversion to the octahedral form, with the intensity of the transition ν_3 [${}^3\text{T}_1 \rightarrow {}^3\text{T}_1(\text{P})$] at 17 400/19 330 cm^{-1} for tetrahedral nickel(II) being negligibly small. Upon concentration of the solution, a yellow solid crystallized and was found to be an isopropyl alcohol adduct of compound **1**. The analytical data of the isolated product are consistent with the composition of **4**, which was corroborated by a single-crystal X-ray diffraction study.



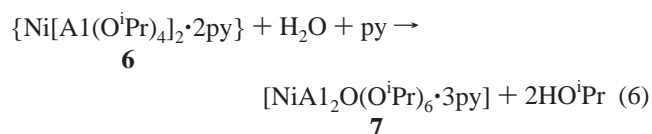
By application of a dynamic vacuum (10^{-3} mbar), compound **4** readily released 2 equiv of isopropyl alcohol and was quantitatively converted to **1** (eq 3). In this way, compound **1** was isolated as a crystalline solid in a pure form. Unfortunately, no suitable crystal could be selected for a single-crystal X-ray diffraction study. It is noteworthy to mention that the crystalline state was not stable, and under storage, the compound started slowly to “melt”. The gradual liquefaction of compound **1**, which proceeded each time at ordinary room temperature, can be regarded as further evidence for the decomposition of the pure substance toward the equilibrium state according to eq 2a. A similar behavior was also observed for the later runnings obtained by fractional distillation, which is to be expected from the above-mentioned equilibrium. On fractionation, the forerunnings contained a significant surplus of aluminum isopropoxide. Because of the gradual enrichment of the distilland with **3**, equilibrium (2a) was continuously shifted to the left and the further runnings gave a pure product, which crystallized spontaneously and remained solid for several hours before liquefaction.

The adduct **5** was obtained by the equimolar reaction of **1** and pyridine as a viscous yellow mass, which slowly crystallized under storage (eq 4). The pyridine donor molecule is strongly bonded to the Ni atom and cannot be removed in vacuum at room temperature. Upon heating under reduced pressure, **5** partly distilled and partly decomposed to pyridine and **1**.

The dissolution of **1** in an excess of pyridine (eq 5) produced a green solution, which on concentration gave the bipyridine adduct **6** as large green crystals, which lost their crystallinity upon removal of the mother liquor. In dynamic vacuum, **6** eliminated a molecule of pyridine and was converted to **5**.



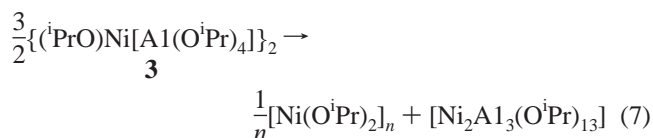
The hydrolysis of compound **6** resulted in the formation of the oxoalkoxide **7**, which crystallized as a light-blue solid (eq 6). Surprisingly, the addition of a stoichiometric amount of water to a solution of **6** in pyridine did not lead to complete conversion to **7**. For X-ray and elemental analysis, suitable crystals were separated from the product mixture.



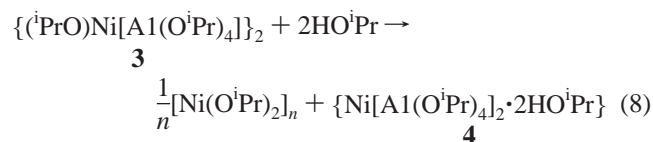
The dimeric nature of **3** in the vapor phase was established by mass spectrometry. Compound **3** is soluble in nonpolar solvents, but the partial removal of the solvent from such

(12) (a) Kleinschmidt, D. C.; Shiner, V. J., Jr.; Whittaker, D. *J. Org. Chem.* **1973**, *38*, 3334–3337. (b) Turova, N. Ya.; Kozunov, V. A.; Yanovskii, A. I.; Bokii, N. G.; Struchkov, Yu. T.; Tarnopolskii, B. L. *J. Inorg. Nucl. Chem.* **1979**, *41*, 5–11.

solutions did not lead to the formation of crystals. Cryoscopic measurements showed that the molecular association of compound **3** in cyclohexane lies at 2.2, which indicates the formation of further oligomeric species. In benzene, the degree of oligomerization increases. Upon cooling a solution of **3** in benzene to the freezing point of the solvent, a blue solid precipitated, whereby the remaining soluble substance in the solution exhibited a molecular association degree of 2.8 with respect to the monomeric unit of **3**, which corresponds to the empirical formula $\text{Ni}_2\text{Al}_3(\text{O}^i\text{Pr})_{13}$. This observation could be regarded as evidence for the existence of further species containing $\text{Ni}(\text{O}^i\text{Pr})_2$ and $\text{Al}(\text{O}^i\text{Pr})_3$ units in various stoichiometric ratios. Equation 7 gives a possible explanation of the behavior of compound **3** in freezing benzene. The hypothetical species $[\text{Ni}_2\text{Al}_3(\text{O}^i\text{Pr})_{13}]$ was not isolated, but the corresponding magnesium compound $[\text{Mg}_2\text{Al}_3(\text{O}^i\text{Pr})_{13}]$ is known and has been structurally characterized.¹³

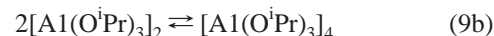
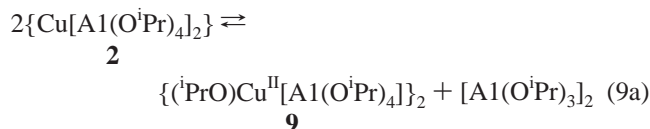


1 forms crystalline adducts with donor solvents, whereas **3** is not stable and decomposes in the presence of the latter. The addition of isopropyl alcohol or pyridine to a solution of **3** in cyclohexane resulted in the precipitation of a blue solid with analytical data corresponding to the formula $\text{Ni}(\text{O}^i\text{Pr})_2$. The quantitative analysis of the precipitate is in agreement with eq 8.

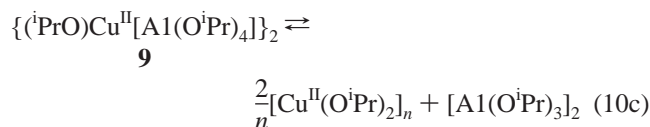
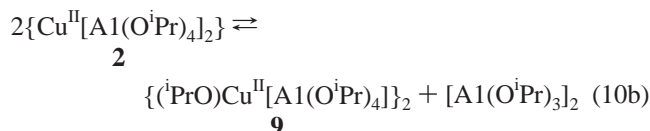
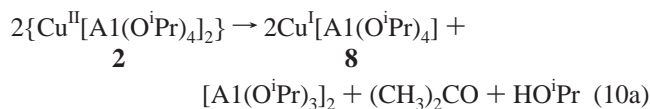


The copper compound **2** is a metastable viscous liquid. The stoichiometric composition $\text{CuAl}_2(\text{O}^i\text{Pr})_8$ of a freshly prepared sample was confirmed by elemental analysis. Moreover, the magnetic moment $\mu_{\text{eff}} = 1.75 \mu_{\text{B}}$ is comparable with the spin-only value ($1.73 \mu_{\text{B}}$), indicating divalent copper. However, NMR spectroscopy revealed that the oil contained approximately 15% $\text{Al}(\text{O}^i\text{Pr})_3$. Upon aging at ambient temperature, the color of the oil changed slowly from bluish green to green. This process was accompanied by the precipitation of a white solid, which was analyzed as **8**, and the formation of colorless $[\text{Al}(\text{O}^i\text{Pr})_3]_4$ crystals. After separation of the solids, the filtered oil was stored for several months before further filtration. The storage and filtration steps were repeated several times over a period of 3 years. Finally, a blue solid slowly crystallized out from the filtered green liquid. Surprisingly, the single-crystal diffraction analysis revealed another stoichiometry for the blue compound, namely, **9**. These observations give rise to equilibria (eq 9a,b) similar to the corresponding nickel compound **1**.

Obviously, the solidification of tetrameric aluminum isopropoxide is the driving force for this transformation.



The decomposition of **2** upon distillation is more complex compared to the nickel derivative **1** (eq 10a–c). The analysis of the volatiles by mass spectrometry coupled with the distillation apparatus revealed as the main products isopropyl alcohol and acetone, indicating a partial reduction of copper(II) to copper(I). This finding was also confirmed by NMR analysis of the products isolated in a cooling trap. The isopropyl alcohol to acetone ratio being 2.4 is significantly higher than that expected from eq 10a. The high yield of alcohol suggests a radical-based mechanism for this reaction. The first step requires homolytic scission of a Cu–O bond followed by generation of isopropyl alcohol from the initially formed isopropoxy radical by capturing a H atom from another isopropoxy group. An analogous mechanism has been proposed for the thermal decomposition of some copper(I) alkoxides by Whitesides and co-workers.¹⁴

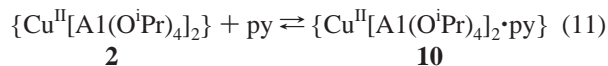


The blue distillate was not stable, and after a while, a white solid precipitated, which was found to be **8**. During storage for several weeks, the color of the distillate changed slowly from blue to green and colorless crystals of tetrameric aluminum isopropoxide were formed. Treatment of the compound mixture with pyridine formed three sorts of crystals, which were analyzed by X-ray diffraction: blue crystals of **10**, pale-yellow ones of **11**, and colorless crystals of $[\text{Al}(\text{O}^i\text{Pr})_3]_4$. Treatment of a nondistilled sample of **2** with pyridine gave mainly **10** (eq 11), which was accompanied only by small amounts of **11** and aluminum isopropoxide. On the contrary, after heating of **2** dissolved in pyridine, **10** failed to crystallize. As confirmed by NMR spectroscopy, the heating induced nearly quantitative reduction of copper(II) to copper(I). The isopropyl alcohol/acetone ratio being 1.9 supports the assumption of a radical-based mechanism.

(13) Meese-Marktscheffel, J. A.; Fukuchi, R.; Kido, M.; Tachibana, G.; Jensen, C. M.; Gilje, J. W. *Chem. Mater.* **1993**, 5, 755–757.

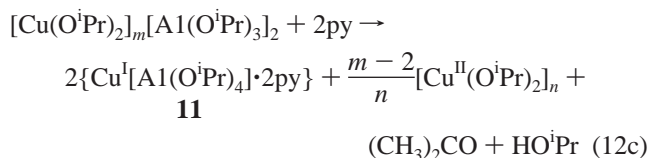
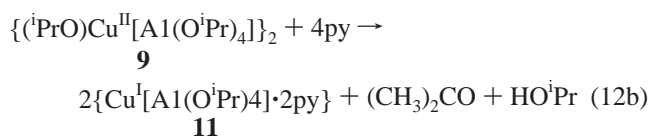
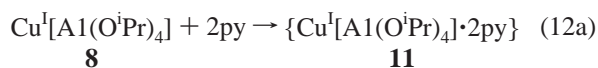
(14) Whitesides, G. M.; Sadowski, J. S.; Lilburn, J. *J. Am. Chem. Soc.* **1974**, 96, 2829–2835.

The tendency of the copper(II) alkoxides to decompose to copper(I) alkoxides appears to depend on the temperature and the polarity of the medium.

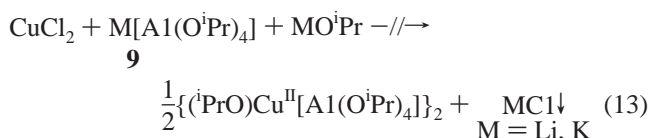


The green residue obtained after evaporation was partly soluble in toluene, and the addition of hot pyridine caused precipitation of a green solid, which was analyzed to be the homometallic copper(II) isopropoxide. Evaporation of the solvent from the filtered pyridine solution gave only crystals of complex **11**.

8 was partly present in the distillate because of its poor volatility, but its main amount was found in the distillation residue among **9** and $[\text{Cu}(\text{O}^i\text{Pr})_2]_n$, both species of the type $[\text{Cu}(\text{O}^i\text{Pr})_2]_m[\text{Al}(\text{O}^i\text{Pr})_3]_2$ (where $m > 2$). The species $[\text{Cu}(\text{O}^i\text{Pr})_2]_m[\text{Al}(\text{O}^i\text{Pr})_3]_2$ could be either molecular species or colloidal $\text{Cu}(\text{O}^i\text{Pr})_2$ particles stabilized with aluminum isopropoxide on the surface, which makes them soluble in nonpolar solvents. The treatment of the distillation residue with pyridine transformed **8** into **11** according to eq 12a. Heating of the solution accelerated the decomposition of **9**, and the species of the type $[\text{Cu}(\text{O}^i\text{Pr})_2]_m[\text{Al}(\text{O}^i\text{Pr})_3]_2$ to **11** as proposed in eq 12b,c was formed, which was accompanied by the precipitation of $\text{Cu}^{\text{II}}(\text{O}^i\text{Pr})_2$. After filtration and evaporation of the solvent from the solution, compound **11** was the only substance that was isolated.



Attempted preparation of **9** by reaction between either CuCl_2 , $\text{Li}[\text{Al}(\text{O}^i\text{Pr})_4]$, and LiO^iPr or CuCl_2 , $\text{K}[\text{Al}(\text{O}^i\text{Pr})_4]$, and KO^iPr in equimolar proportions failed (eq 13). In the first case, nearly quantitative reduction of copper(II) to copper(I) occurred, whereas the second route resulted in the formation of **2** and $[\text{Cu}(\text{O}^i\text{Pr})_2]_n$. The failure to prepare **9** via the second route could be due to its instability in isopropyl alcohol.



Reactions of $\{\text{M}[\text{Al}(\text{O}^i\text{Pr})_4]_2\}$ [$\text{M} = \text{Ni}^{\text{II}}$ (**1**) and Cu^{II} (**2**)] with various alcohols have been reported so far in the literature.^{6a,b} Mehrotra and co-workers described that in the

case of *tert*-butanol only six out of eight isopropoxy groups could be replaced by *tert*-butoxy groups. In the course of our study, we repeated these reactions in order to elucidate the structural features of the derivatives of the type $[\text{MAl}_2(\text{O}^i\text{Pr})_{8-\alpha}(\text{O}^t\text{Bu})_\alpha]$, where $\text{M} = \text{Ni}^{\text{II}}$ and Cu^{II} .

2 was allowed to react at room temperature with an excess of *tert*-butanol in toluene. After removal of the solvent under reduced pressure, the procedure was repeated several times. The progress of the reaction was followed by the determination of the isopropyl alcohol liberated in each step. The first step resulted only in the partial replacement of approximately two isopropoxy groups. The lower substituted derivatives $[\text{Cu}^{\text{II}}\text{Al}_2(\text{O}^i\text{Pr})_{8-\alpha}(\text{O}^t\text{Bu})_\alpha]$ ($\alpha < 4$) form bluish-green oils. Further replacement of the isopropoxy groups by *tert*-butoxy groups led to solidification and to a change in the color to green. Because the starting material **2** is always a mixture of compounds, the final product of the alcoholysis reaction was also a complicated mixture of various types of species. After sublimation, the mixture was dissolved in toluene, and the insoluble copper(I) alkoxides $\text{Cu}^{\text{I}}\text{Al}(\text{O}^i\text{Pr})_{4-\gamma}(\text{O}^t\text{Bu})_\gamma$ ($\gamma = 1-4$) were removed by filtration. After evaporation of the solvent, the other compounds were separated by fractional sublimation. A white sublimate containing aluminum alkoxide species of the type $[\text{Al}_2(\text{O}^i\text{Pr})_{6-\delta}(\text{O}^t\text{Bu})_\delta]$ ($\delta = 5-6$) was obtained at 80 °C. A mixture of various derivatives $[\text{Cu}^{\text{II}}\text{Al}_2(\text{O}^i\text{Pr})_{8-\alpha}(\text{O}^t\text{Bu})_\alpha]$ ($\alpha \leq 6$) was collected at 100 °C. Finally at 120 °C, the last crop contained **12**, as confirmed by elemental and X-ray diffraction analysis. Compound **12** is thermally stable and sublimes without leaving any solid residues.

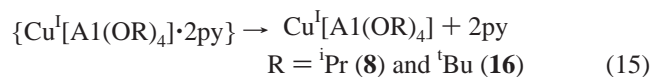
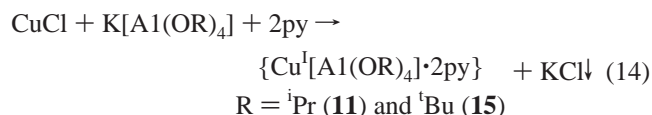
The reaction of **1** and **4** with an excess of *tert*-butanol was also examined briefly. In contrast to **2**, the replacement of the isopropoxy groups occurred quite readily at ambient temperature and **13** was obtained in a quantitative yield. The product was sublimed unchanged under reduced pressure. The expected composition was confirmed by elemental and X-ray analysis. In contrast to **1**, derivative **13** is stereochemically rigid and shows a tendency neither to form adducts with alcohol nor to undergo thermal decomposition.

The bimetallic *tert*-butoxide **14** was obtained in analogy to eq 1, reacting anhydrous CuCl_2 with $\text{K}[\text{Al}(\text{O}^t\text{Bu})_4]$ in a toluene/*tert*-butanol solution following a procedure already described in the literature.^{5b} After removal of the precipitated KCl and evaporation of the solvent, a green solid formed. Apart from **14**, the crude product of the reaction contained $[\text{Al}(\text{O}^t\text{Bu})_3]_2$ and further copper(II) species, which were not volatile. $[\text{Al}(\text{O}^t\text{Bu})_3]_2$ (80 °C and 10^{-2} mbar) and **14** (120 °C and 10^{-2} mbar) were separated from the green residue by fractional sublimation. In contrast to the observations made by Mehrotra and co-workers, who describe the compound as a green, sticky solid, upon distillation at 162 °C and 0.05 Torr, we got **14** as a yellow crystalline solid. Elemental analysis and X-ray structure determination confirmed the composition as $\text{CuAl}_2(\text{O}^t\text{Bu})_8$. The ^1H NMR spectrum of **14** displays at room temperature a single resonance for the methyl protons of the O^tBu groups. However, the intensity of the signal (in a ratio to the solvent resonances) corresponds to four O^tBu groups and probably

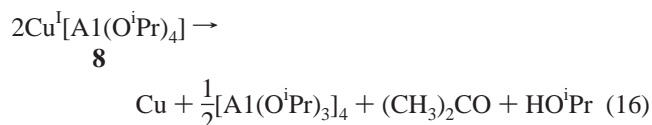
originates from the terminal alkoxy groups located far away from the paramagnetic center.

11 was initially obtained by the treatment of **2** with pyridine. Interestingly, the efforts made to synthesize **14** by the reaction of CuCl_2 and $\text{K}[\text{Al}(\text{O}^i\text{Bu})_4]$ in the presence of pyridine also resulted in the formation of the corresponding *tert*-butoxide derivative **15**. Consequently, it appears that pyridine favors the reduction of copper(II) to copper(I).

The preparation of **8** by a simple metathesis reaction was not successful. Because of its poor solubility in common organic solvents, **8** could not be separated from the precipitated KCl. The addition of pyridine led to the dissolution of the double isopropoxide as **11**, which was obtained after the workup of the reaction mixture (eq 14). An analogous procedure was employed for the preparation of **15**. Both compounds were characterized by elemental analysis, NMR spectroscopy, and single-crystal structure determination. Compound **15** in a toluene solution is slowly reacting with air (oxygen and water) to form the decomposition product **17**, which has been characterized by X-ray diffraction on single crystals (see below).



Upon heating under reduced pressure (80 °C and 10^{-2} mbar), **11** released pyridine and **8** was formed (eq 15). Attempted sublimation initially delivered **8** in a rather low yield (13%) as a white sublimate. However, prolonged heating of **8** in vacuum (120 °C and 10^{-2} mbar) resulted in decomposition, forming mostly aluminum isopropoxide and metallic copper (eq 16). Consequently, **8** cannot be purified by sublimation. The dimeric nature of **8** in the vapor phase was established by mass spectrometry. Its molecular weight could not be determined cryoscopically because of its insufficient solubility in benzene and cyclohexane. In the solid state, it probably has a polymeric structure.



Alternatively, **2** can be used as a starting source for the preparation of **8** according eq 10a. Prolonged refluxing of **2** in vacuum yielded **8** as a nearly colorless residue in the receiver flask. The pale-green color of the product was due to some $[\text{Cu}(\text{O}^i\text{Pr})_2]_n$ impurities.

Efforts made to prepare copper(I) aluminum *tert*-butoxide by either Lewis acid–base adduct formation (eq 17) or metathesis reaction (eq 18) were not successful. $[\text{Al}(\text{O}^t\text{Bu})_3]_2$ and $[\text{CuO}^t\text{Bu}]_4$ did not react in boiling toluene. The addition of polar solvents such as *tert*-butanol, monoglyme, or dioxane and prolonged refluxing of the reaction mixture for several days resulted only in the formation of small quantities of **16**

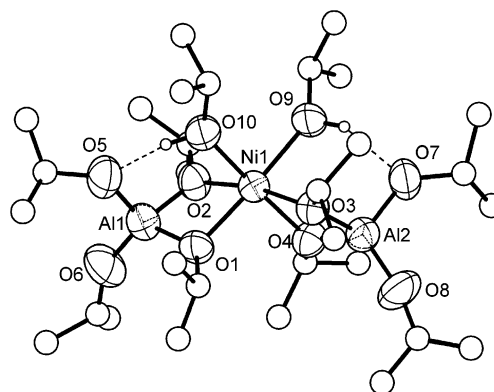
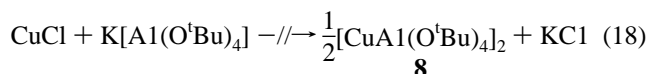
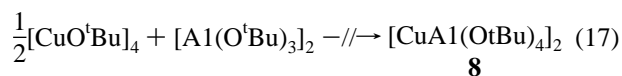


Figure 1. Graphical representation of **4**, ellipsoids showing 50% probability. As in the following figures, the C atoms are represented as simple balls; H atoms are omitted for clarity.

as found from NMR experiments. Anhydrous copper(I) chloride did not react with $\text{K}[\text{Al}(\text{O}^t\text{Bu})_4]$ even under reflux. The addition of pyridine and *tert*-butanol facilitated both reactions, and **14** was obtained in a quantitative yield. On heating under reduced pressure, **14** released 2 equiv of pyridine and **16** was formed (eq 15). The sublimation of **16** in vacuum (120 °C and 10^{-2} mbar) was accompanied by decomposition, leaving some residue. Analytically pure product was, nevertheless, obtained upon recrystallization of the sublimate from hot toluene. The composition $[\text{CuAl}(\text{O}^t\text{Bu})_4]_2$ was confirmed by crystal structure determination.



Molecular and Solid-State Structures

A collection of the experimental setup and the most important data concerning the X-ray diffraction analyses are compiled in Tables 1 and 2. Selected bond lengths and angles are summarized in Tables 3 and 4.

Compound 4. Figure 1 shows a graphic representation of the molecular structure of **4** derived from a single-crystal X-ray diffraction analysis. The pertinent bond lengths and angles are compiled in Table 3. The structure of **4** (almost point symmetry C_2) is analogous to the corresponding magnesium compound $\{\text{Mg}[\text{Al}(\text{O}^i\text{Pr})_4]_2 \cdot 2^i\text{PrOH}\}^{15}$ and consists of two aluminum-centered oxygen tetrahedra sharing common edges with a nickel-centered octahedron. Apart from the O atoms of the AlO_4 tetrahedra, the fifth and sixth coordination sites of the Ni atom are occupied by the O atoms of the solvating isopropyl alcohol molecules, located in cis position with respect to each other. The central Ni atom is substantially distorted from the regular octahedral geometry with trans O–Ni–O angles ranging from 168.6° to 175.9° and cis angles in the range from 73.0° to 103.0°. The Ni–O distances from the neutral alcohol ligands [ave 2.102(7) Å] are larger than the bridging Ni–O distances [ave 2.045(6)

(15) Sassmannshausen, J.; Riedel, R.; Pflanz, K. B.; Chmiel, H. Z. *Naturforsch.* **1993**, 48b, 7–10.

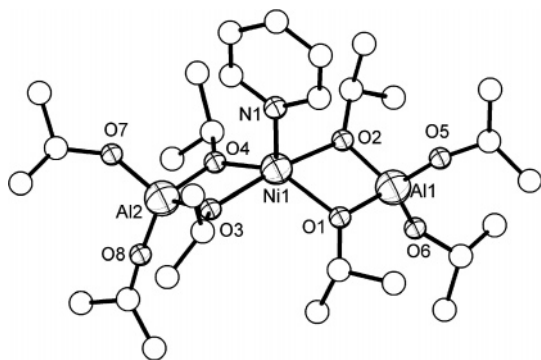


Figure 2. Graphical representation of **5**, ellipsoids showing 50% probability (see also Figure 1).

Å] because of the reduced donor capacity of the alcohol in comparison to the charged alkoxo ligands.

The hydroxylic H atoms on O9 and O10 participate in intramolecular hydrogen bonding with the terminal alkoxy ligands (O7 and O5) evident in the short $O9 \cdots O7 = 2.696$ Å and $O10 \cdots O5 = 2.695$ Å separations (sum of O van der Waals radii = 3.00 Å).¹⁶ These hydrogen bridges result in the formation of six-membered chelate cycles [Ni- μ_2 -O-Al-O \cdots H-O] fused with the four-membered NiO₂Al rings, causing further stabilization of the molecule.

The aluminum centers are in a distorted tetrahedral environment. The Al-O bond lengths are comparable with those observed for {Mg[Al(OⁱPr)₄]₂·2HOⁱPr} and follow the trend Al-O_{term} [ave 1.636(9) Å] < Al-O_{term} [involved in intramolecular hydrogen bonding; ave 1.708(8) Å] < Al-O_{bridge} [ave 1.757(7) Å]. The bridging O atoms are almost planar [average sum of angles = 357.9(5)°], accounting for sp² hybridization.

Compound 5. The molecular structure of **5**, which has almost point group symmetry *C*₂ (with the quasi *C*₂ axis intersecting the pyridine ligand), consists of two planar AlO₂-Ni four-membered rings [sum of angles = 360.0(2)°] joined at the Ni atom to which a pyridine molecule is bonded through the N atom. The nickel coordination figure NiO₄N can be described as a distorted trigonal bipyramid with a bending of the axial O2-Ni-O3 angle from the ideal 180° to 169.5(2)°. In Figure 2, the central NiAlON backbone of the structure is shown, omitting all H atoms for clarity; some important bond lengths and angles are assembled in Table 3. The two doubly bridging OⁱPr groups of each [Al(OⁱPr)₄] unit are bonded to the nickel center in an asymmetrical fashion with short equatorial Ni-O1 and Ni-O4 distances [ave 1.993(3) Å] and larger axial Ni-O2 and Ni-O3 distances [ave 2.055(3) Å]. The mean Ni-O bond length in **5** is 2.023(3) Å for the pentacoordinate Ni atom compared to 2.064(7) Å for the hexacoordinate Ni atom in **4**. The bonding angles within the NiO₂Al rings of the two compounds are similar, being in **4** more acute at the nickel and aluminum centers because of the higher coordination number of nickel [73.0(3)° (**4**) in comparison with 74.5(1)° (**5**)]. As expected, the terminal Al-O bond lengths of ave 1.668(5) Å are shorter than the bridging ones [ave 1.771(4) Å].

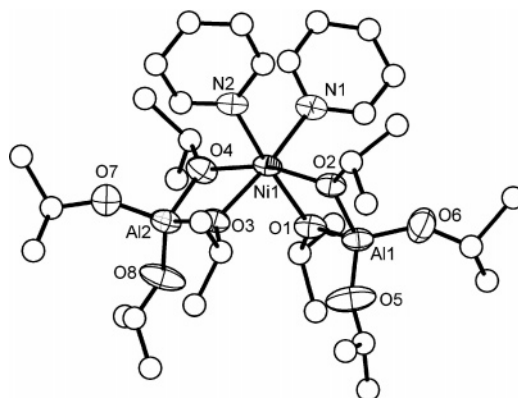


Figure 3. Graphical representation of **6**, ellipsoids showing 50% probability from a preliminary structure determination (see also Figure 1).

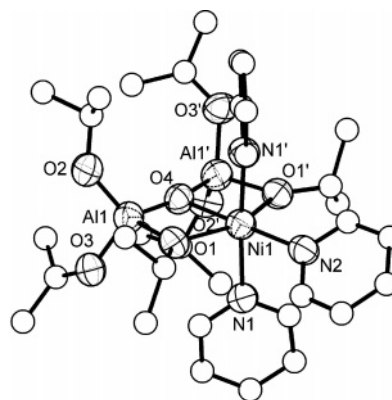


Figure 4. Graphical representation of **7**, ellipsoids showing 50% probability (see also Figure 1).

Compound 6. An attempted X-ray structure determination of **6** did not lead to a satisfactory solution because of the poor quality of the crystals. An appreciable residual electron density prevented the completion of the refinement. The preliminary solid structure model exhibits a primitive triclinic cell with two independent molecules in the asymmetric unit. The most important feature of the structure (Figure 3) is its similarity to the structure of **4**. Apart from the two bidentate [Al(OⁱPr)₄] ligands, two solvating pyridine molecules situated in cis position toward each other fill in the octahedral coordination environment around the Ni atom.

Compound 7. The central core of **7** (compare Figure 4) is built up of two planar NiO₂Al four-membered rings fused along the common Ni- μ_3 -O edge. The rings are coplanar because of the requirements of the twofold symmetry axis in the crystal passing through O4, Ni, N2, and C17. The three N atoms of the pyridine molecules and the two bridging alkoxy and oxo O atoms form a distorted octahedron around the nickel center. Bond lengths and angles at the Ni atom are comparable with those of compounds **4** and **5** (see also Table 4). All bridging O atoms have trigonal-planar surroundings [sum of angles 360.0(3)°]. The coordination figure around the O4 atom bridging the nickel and the two Al atoms [O4-Al = 1.676(1) Å; O4-Ni = 1.990(4) Å] is trigonal-planar with a remarkable tendency of the Al1-O4-Al1a angle to linearity [166.1(3)°], which could result from steric reasons. The different functions of the O atoms in the structure (oxo, bridging, and terminal alkoxy) are reflected

(16) Bondi, A. J. *Phys. Chem.* **1964**, 68, 441–451.

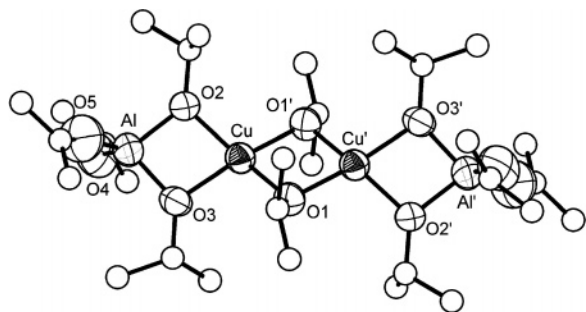


Figure 5. Graphical representation of **9**, ellipsoids showing 50% probability (see also Figure 1).

by a considerable difference in the Al–O values (respectively 1.676(2), 1.633(3), and 1.726(3) Å).

Compound 9. The crystal structure of **9** (Figure 5) contains centrosymmetric dimeric molecules of the general formula $\{(\text{iPrO})\text{Cu}[\text{Al}(\text{O}^i\text{Pr})_4]\}_2$. The backbone of the structure is made up of a planar Cu_2O_2 rhombus connected with two planar CuO_2Al four-membered rings [sum of angles = $359.99(13)^\circ$] through the Cu atoms. The distances within the central Cu_2O_2 four-membered ring [Cu–O = ave 1.920(3) Å, Cu···Cu = 2.898(1) Å, and O···O = 2.519(3) Å] are quite similar to the distances found in compound **17** (see below) containing a $\text{Cu}^{\text{II}}_2(\text{OH})_2$ unit [Cu–O(1) = 1.925(7) Å, Cu···Cu = 2.989(2) Å, and O···O = 2.465(2) Å]. The bonding angles O1–Cu–O1' within the Cu_2O_2 four-membered rings of the two compounds are similar, being in **9** somewhat larger at the copper centers because of the lower coordination number of copper [$81.97(12)^\circ$ (**9**) in comparison with $78.2(4)^\circ$ in **17**]. The coordination polyhedron around the Cu atoms in **9** can be described as an extremely flattened tetrahedron not far away from square-planar geometry. The degree of bisphenoidic distortion could be expressed through the angle between the Cu_2O_2 and CuO_2Al planes [$32.23(14)^\circ$]. This value lies far away from 90° , which is expected for an ideal tetrahedron. The extent of tetrahedral compression can be seen as a compromise between the mutual repulsion of the ligands and the crystal-field stabilization of the square-planar geometry. The subsequent replacement of the space-filling *tert*-butoxy by the smaller isopropoxy groups in a $\text{Cu}(\text{OR})_4$ tetrahedron (R = ^tBu and ^iPr) decreases the repulsion of the ligands, and the geometry is shifted toward the square-planar one. For the plane angles between the CuO_2Al planes in **14** and **12** or respectively between the Cu_2O_2 and CuO_2Al planes in **9**, the following dispersion was observed: 77.77° for $\text{Cu}(\text{O}^i\text{Bu})_4$ in **14**, 68.54° for $\text{Cu}(\text{O}^i\text{Pr})_2(\text{O}^i\text{Bu})_2$ in **12**, and 32.23° for $\text{Cu}(\text{O}^i\text{Pr})_4$ in **9**. The distances between O atoms and fourfold-coordinated Cu atoms in **9** [ave 1.941(9) Å] are comparable with the average Cu–O bond lengths of 1.922(5) and 1.933(5) Å in **12** and **14**, respectively.

The Al atoms exhibit a distorted tetrahedral environment, with O–Al–O angles ranging from $85.1(1)^\circ$ to $116.4(2)^\circ$. The expected dispersion of Al–O bond lengths in **9** [Al–O_{term} = ave 1.680(4) Å < Al–O_{bridg} = ave 1.794(4) Å] is quite similar to that found in **10** [Al–O_{term} = ave 1.691(10) Å and Al–O_{bridg} = ave 1.798(8)].

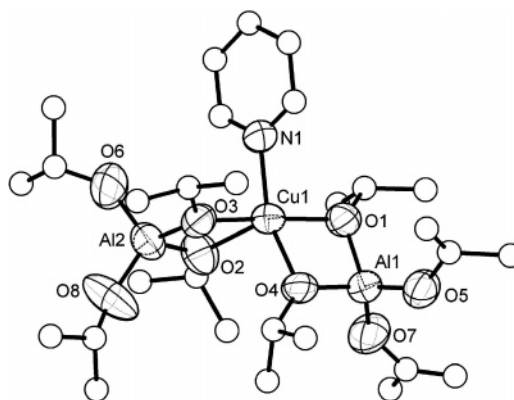


Figure 6. Graphical representation of **10**, ellipsoids showing 50% probability (see also Figure 1).

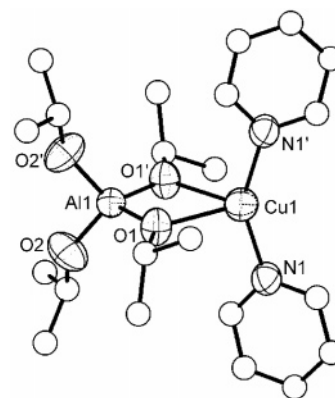


Figure 7. Graphical representation of **11**, ellipsoids showing 50% probability (see also Figure 1).

Compound 10. It is interesting to compare the solid-state molecular structure of **10** (Figure 6) with the corresponding one of the nickel compound **5** (Figure 2). Whereas the two bidentate $[\text{Al}(\text{O}^i\text{Pr})_4]^-$ ligands in **5** are bonded to the nickel center nearly symmetrically with respect to the quasi twofold axis C_2 passing through the Ni–N bond, in **10** the two crystallographic inequivalent $[\text{Al}(\text{O}^i\text{Pr})_4]^-$ units are coordinated to copper in an asymmetrical fashion. One of the Cu–O bonds is about 0.36 Å longer than the others [Cu–O2 = 2.327(8) Å in comparison with Cu–O3 = 1.962(6) Å, Cu–O1 = 1.963(6) Å, and Cu–O4 = 1.985(6) Å]. The NO_3 coordination polyhedron around copper can be described as a distorted tetragonal pyramid consisting of one N atom and three strongly bonded O atoms in its base and a bridging O atom at the apex. As may be seen by inspection of Table 3, this description is in accordance with the observed bond lengths and angles.

Compounds 11 and 15. The solid-state structure of **11** (see also Figure 7 and Table 3 for distances and angles) is built up of monomeric molecules in which Cu, Al, and two bridging O atoms form a strictly planar four-membered ring with a crystallographic twofold symmetry axis C_2 passing through Cu and Al. The coordination figure around Cu can be described as an extremely distorted N_2O_2 tetrahedron with two short Cu–N bonds [1.945(4) Å in comparison to the longer Cu–N bond of 2.046 Å in $[\text{Cu}^{\text{I}}(\text{py})_4]\text{ClO}_4$ ¹⁷ forming a large N1–Cu–N1a angle of $145.9(3)^\circ$. The small O1–Cu–O1a angle of $67.0(2)^\circ$ at the tetrahedral copper in **11** is

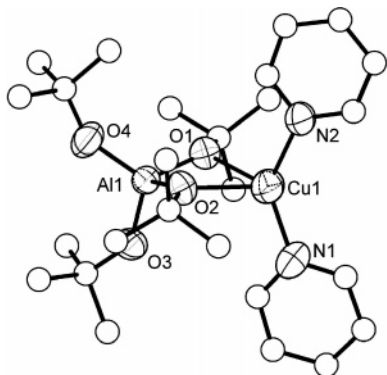


Figure 8. Graphical representation of **15**, ellipsoids showing 50% probability (see also Figure 1).

associated with extremely large Cu–O distances [2.312(3) Å in **11** in comparison with the mean Cu–O distance of 1.886(2) Å in **15**]. This situation suggests increased ionic character of the bonds between the Cu and O atoms. Therefore, compound **11** can be better described as an ion pair of the type $[\text{Cu}(\text{py})_2]^+[\text{Al}(\text{O}^i\text{Pr})_4]^-$ with quite strong $\text{Cu}^+\cdots\text{O}^i\text{Pr}$ interactions and a tendency of the N–Cu–N angle to become linear. On the same line, all isopropoxy groups at the Al atom are essentially terminal, which is evident in the small difference between the terminal and bridging OⁱPr groups [$\text{Al}–\text{O}_{\text{term}} = 1.718(4)$ Å in comparison with $\text{Al}–\text{O}_{\text{bridg}} = 1.736(3)$ Å]. The ambient-temperature ¹H and ¹³C NMR spectra show only one type of isopropoxide environment owing to the fluxional behavior of this ligand in solution.

As shown in Figure 8, the molecular structure of **15** is similar to the structure of **11**, but the two substances are not isostructural. The central four-membered CuO₂Al ring in **15** is not planar, and the tetrahedral coordination environment around copper is not as extremely distorted as that in **11**. The Cu–O distance of 2.239(3) Å is still significantly larger than the sum of the effective ionic radii of Cu⁺ and O²⁻ (1.96 Å)¹⁸ but considerably shorter than the Cu–O bond length in **11** [2.312(3) Å] because of the increase in covalency of the Cu–O bond. This is also associated with subsequent elongation of the Cu–N bonds [ave 1.958(4) Å] and a decrease in the value of the N–Cu–N bond angle [137.3(2)°]. The closer attachment of $[\text{Cu}(\text{py})_2]^+$ to two of the O atoms of the $[\text{Al}(\text{O}^i\text{Bu})_4]^-$ anion lengthens the Al–O_{bridg} bonds by 0.046 Å compared to the terminal ones. The difference in the structures of **11** and **15** may be attributed to the higher inductive effect of *tert*-butyl compared to isopropyl, with the oxygen getting more electron density in the *tert*-butyl case.

Compound 16. The X-ray structural study of **16** reveals the crystal to be built up of dimeric centrosymmetric molecules, which have two $[\text{Al}(\text{O}^i\text{Bu})_4]$ units linked by two nearly linear O–Cu–O bridges [176.44(7)°] to form an eight-membered ring in a chairlike conformation (Figure 9).

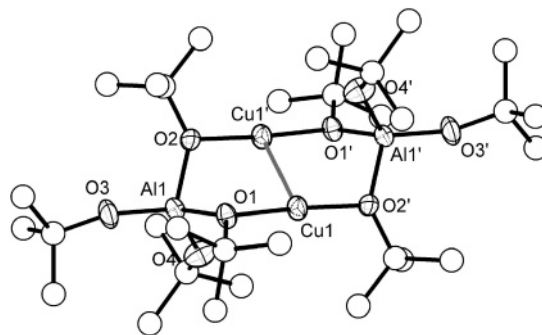


Figure 9. Graphical representation of **16**, ellipsoids showing 50% probability (see also Figure 1).

A similar structural pattern was observed in $[\text{CuN}(\text{SiMe}_2\text{NEt}_2)_2]_2$ containing a $(\text{CuNAlN})_2$ eight-membered ring with linearly coordinated Cu^I atoms.¹⁹

The short Cu^I⋯Cu^I separation of 2.687(1) Å, which is smaller than the sum of the van der Waals radii (2.80 Å), not only results from the small bite distance of the $[\text{Al}(\text{O}^i\text{Bu})_4]^-$ ligands. Moreover, the bending of the two O–Cu–O bridges toward each other is indicative of a very weak metal–metal bonding caused both by weak dispersion attraction between the filled 3d¹⁰ electron shells of the Cu⁺ ions and by a decrease of Pauli repulsion of the outer electron shells by hybridization between 3d, 4s, and 4p orbitals.²⁰ The average Cu–O bond length of 1.886(2) Å, which is comparable with the Cu–O distances in other copper alkoxides [1.852 Å in $[\text{Cu}(\text{O}^i\text{Bu})_4]$ ²¹ and 1.840 Å in $[\text{LiCu}(\text{O}^i\text{Bu})_2]$ ²²], indicates a covalent bonding between the Cu and O atoms. Consequently, the geometry at the O atoms of the bridging OⁱBu groups deviates from planarity, as shown by the sum of their interbond angles [352.3(1)° for O1 and 357.6(2)° for O2].

Compounds 12–14. As is evident from the unit cell parameters and atomic coordinates, the copper aluminates **14** and **12** are isomorphous and crystallize in the same space group. Furthermore, **14** and **12** are isostructural with the corresponding cobalt, nickel, and magnesium compounds.^{7c,23}

The molecular structures of **14** and **12** display a spirocyclic core made up of two almost planar CuO₂Al four-membered rings joined at the copper center (Figures 10 and 11). Both copper and aluminum atoms are quasi-tetrahedrally coordinated by the alkoxy ligands, with the distortion being more significant at the copper center. The deviation from the ideal tetrahedral geometry can be expressed in terms of distortions with respect to the *S*₄ symmetry axes of an ideal CuO₄ tetrahedron. The elongation along the molecular Al–Cu–Al axis is caused by the small O–Al–O bite of the tetraalkoxyaluminate ligands. On the other hand, the CuO₄ tetrahedra are somewhat flattened as a result of a bisphe-

(17) Nilsson, K.; Oskarsson, A. *Acta Chem. Scand., Ser. A* **1982**, *36*, 605–610.

(18) Huheey, J. E.; Keiter, E. A.; Keiter, R. L. *Inorganic Chemistry: Principles of Structure and Reactivity*, 4th ed.; HarperCollins: New York, 1993; references cited therein.

(19) Koban, A. Ph.D. Thesis, Saarland University, Saarbruecken, Germany, 1999.

(20) Wang, S.-G.; Schwarz, W. H. E. *Angew. Chem., Int. Ed.* **2000**, *39*, 1757–1761.

(21) Greiser, T.; Weiss, E. *Chem. Ber.* **1976**, *109*, 3142–3146.

(22) Purdy, A. P.; George, C. F. *Polyhedron* **1995**, *14*, 761–769.

(23) (a) Wolfanger, H. Ph.D. Thesis, Saarland University, Saarbruecken, Germany, 1991. (b) Fritscher, E. Ph.D. Thesis, Saarland University, Saarbruecken, Germany, 1997.

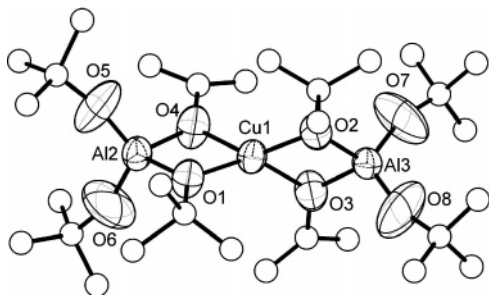


Figure 10. Graphical representation of **12**, ellipsoids showing 50% probability (see also Figure 1).

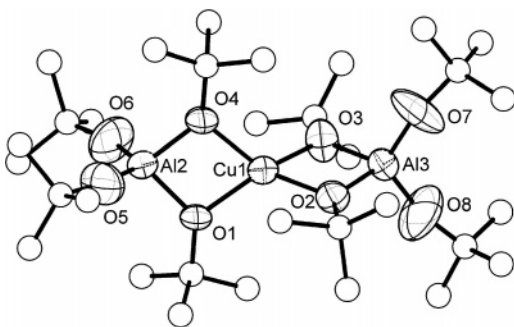


Figure 11. Graphical representation of **14**, ellipsoids showing 50% probability (see also Figure 1).

noidic distortion, which may be due to the Jahn–Teller effect. Whereas the MO_2Al four-membered rings in $\{\text{M}[\text{Al}(\text{O}^t\text{Bu})_4]_2\}$ ($\text{M} = \text{Co}$, Ni , and Mg) are nearly perpendicular to each other (88.7° for $\text{M} = \text{Ni}$ and 88.3° for $\text{M} = \text{Mg}$), the planes of the CuO_2Al rings are twisted toward each other to form smaller angles (77.77° in **14** and 68.54° in **12**).

The degree of the tetrahedral compression can be seen as a compromise between the mutual repulsion of the ligands and the crystal-field stabilization of the square-planar geometry. Therefore, the replacement of two out of the four *tert*-butoxy groups with the less space-filling O^iPr ligands results in a more flattened CuO_4 tetrahedron in **12**. As a result of this, the broad absorption band of the CuO_4 chromophore in **12** at $12\,531\text{ cm}^{-1}$ is shifted toward larger wavenumbers in comparison to **14** ($10\,741\text{ cm}^{-1}$). The distances between O atoms and fourfold-coordinated Cu atoms of ave $1.922(5)$ and $1.933(5)\text{ Å}$ respectively in **12** and **14** are smaller than the average Cu–O bond length of ave 2.059 Å in **10** (square-pyramidal geometry). The expected dispersion of Al–O bond lengths [$\text{Al–O}_{\text{term}} < \text{Al–O}_{\text{bridg}}$] is found in AlO_4 tetrahedra with Al–O_{term} distances of $1.632(8)\text{ Å}$ in **12** and $1.643(7)\text{ Å}$ in **14** and Al–O_{bridg} distances of $1.778(6)\text{ Å}$ in **12** and $1.787(6)\text{ Å}$ in **14**. The same structural pattern was also observed for **13** (Figure 12). Whereas **12**, **14**, $\{\text{Ni}[\text{Al}(\text{O}^t\text{Bu})_4]_2\}$, and $\{\text{Mg}[\text{Al}(\text{O}^t\text{Bu})_4]_2\}$ crystallize in the monoclinic space group $P2_1/n$, **13** crystallizes in the orthorhombic space group $P2_12_12_1$. The two bidentate $[(\mu_2\text{-O}^i\text{Pr})(\mu_2\text{-O}^t\text{Bu})\text{-Al}(\text{O}^t\text{Bu})_2]$ moieties tetrahedrally coordinated to the Ni atom form two almost planar AlO_2Ni four-membered rings [sum of angles = 359.6°] with a plane angle of $89.7(3)^\circ$, which is almost 90° as expected for an ideal tetrahedron. The two possible positions of the two bridging isopropoxy groups with respect to each other along the molecular Al–Ni–Al axis

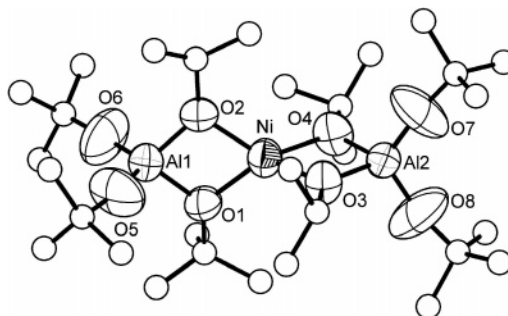


Figure 12. Graphical representation of **13**, ellipsoids showing 50% probability; one of the enantiomeric forms is shown (see also Figure 1).

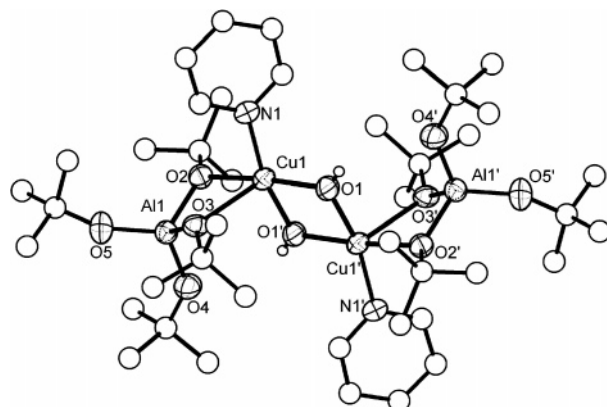


Figure 13. Graphical representation of **17**, ellipsoids showing 50% probability (see also Figure 1).

result in the formation of two geometric isomers sharing the same crystallographic positions in this acentric space group. As a result of this, only the isopropoxy group connected to O2 could be clearly resolved. The other one sharing the same positions with a *tert*-butoxy group was located with approximately 50% occupancy at O3 and O4.

The mean Ni–O bond length in **13** (coordination number 4) being $1.946(7)\text{ Å}$ is smaller than the Ni–O distances in **5** [ave $2.023(3)\text{ Å}$] (coordination number 5) and in **4** [ave $2.064(7)\text{ Å}$] (coordination number 6). The Al–O bond lengths in **13** exhibit the typical dispersion: $\text{Al–O}_{\text{term}} = \text{ave } 1.649(10)\text{ Å} < \text{Al–O}_{\text{bridg}} = \text{ave } 1.790(10)\text{ Å}$.

Compound 17. The crystal structure of **17** (Figure 13) contains centrosymmetric dimers of the general formula $\{(\text{HO})\text{Cu}[\text{Al}(\text{O}^t\text{Bu})_4]\text{py}\}_2$. The backbone of the structure is made up of two CuO_2Al four-membered rings spirocyclically connected through Cu atoms with a central Cu_2O_2 rhombus. Each Cu atom has a further pyridine molecule coordinated, increasing the coordination number at Cu to 5. Distances and angles within the central four-membered ring are quite similar to the Cu–OH distances found in other compounds containing a $\text{Cu}^{\text{II}}_2(\text{OH})_2$ unit (Cu–O1 = 1.925 Å , Cu \cdots Cu = 2.989 Å , and O \cdots O = 2.465 Å).²⁴ The distances between the hydroxylic oxygen O1 and the other O atoms, e.g., O1 \cdots O4 = 3.128 Å , are larger than the sum of O van der Waals radii (3.00 Å), so there is no structural evidence for the existence of intramolecular hydrogen bonding.

Like in **10**, the O atoms of the bridging O^tBu groups of each $[\text{Al}(\text{O}^t\text{Bu})_4]$ unit are asymmetrically bonded to the

copper centers, resulting in extremely different Cu–O bond lengths: Cu–O3 = 2.393(5) Å compared with Cu–O2 = 2.033(5) Å. The distance from the Cu atom to the N atom of the solvating pyridine molecule being 2.016(7) Å is quite similar to the Cu–N bond length of 2.029(8) Å in **10**. The coordination polyhedron around the Cu atom can be described as a square pyramid with a N atom, two hydroxy atoms, and a bridging O atom in its base and with the O3 atom at the apex.

- (24) (a) Kitajima, N.; Fujisawa, K.; Fujimoto, C.; Moro-oka, Y.; Hashimoto, S.; Kitagawa, T.; Toriumi, K.; Tatsumi, K.; Nakamura, A. *J. Am. Chem. Soc.* **1992**, *114*, 1277–1291. (b) Lewis, D. L.; Hatfield, W. E.; Hodgson, D. J. *Inorg. Chem.* **1972**, *11*, 2216–2221. (c) Lewis, D. L.; Hatfield, W. E.; Hodgson, D. J. *Inorg. Chem.* **1974**, *13*, 147–152. (d) Hammond, R. P.; Cavaluzzi, M.; Haushalter, R. C.; Zubieta, J. A. *Inorg. Chem.* **1999**, *38*, 1288–1292. (e) Komaei, S. A.; van Albada, G. A.; Haasnoot, J. G.; Kooijman, H.; Spek, A. L.; Reedijk, J. *Inorg. Chim. Acta* **1999**, *286*, 24–29.

The Al–O bond lengths do not fall into two different categories (terminal–bridging) but follow a more elaborate trend: Al–O5_{term} = 1.707(6) Å < Al–O4_{term} (oriented toward the hydroxylic O1) = 1.725(6) Å < Al–μ₂-O3_{apex} = 1.762(6) Å < Al–μ₂-O2_{base} = 1.828(5) Å.

Acknowledgment. The authors thank the Fonds der Chemischen Industrie and the BASF AG for their financial support and the “Sonderforschungsbereich 277” as well as the “Europäisches Graduiertenkolleg” GRK 532, both financed by the Deutsche Forschungsgemeinschaft (DFG), Bonn, Germany, for the provision of a postdoctoral grant to K.V.

Supporting Information Available: Crystallographic data of the structures in CIF format. This material is available free of charge via the Internet at <http://pubs.acs.org>.

IC701729Y